DISCLAIMER

This report was prepared as an account of work sponsored by an agency of the United States Government. Neither the United States Government nor any agency thereof, nor any of their employees, makes any warranty, express or implied, or assumes any legal liability or responsibility for the accuracy, completeness, or usefulness of any information, apparatus, product, or process disclosed, or represents that its use would not infringe privately owned rights. Reference herein to any specific commercial product, process, or service by trade name, trademark, manufacturer, or otherwise does not necessarily constitute or imply its endorsement, recommendation, or favoring by the United States Government or any agency thereof. The views and opinions of authors expressed herein do not necessarily state or reflect those of the United States Government or any agency thereof. Reference herein to any social initiative (including but not limited to Diversity, Equity, and Inclusion (DEI); Community Benefits Plans (CBP); Justice 40; etc.) is made by the Author independent of any current requirement by the United States Government and does not constitute or imply endorsement, recommendation, or support by the United States Government or any agency thereof.

Floating Solar in Hydropower Reservoirs in the United States

Techno-economics, Environmental Considerations, Regulatory Pathways, and Technical Potential

INL/RPT-25-82657
Revision 0

Solar Energy Technologies Office and Water Power Technologies Office

JANUARY 2026

Juan Gallego-Calderon, Tyler B. Phillips, Mucun Sun, and Tanveer Hussain
Idaho National Laboratory

Aaron Levine, Evan Rosenlib, and Marie Rivers
National Renewable Energy Laboratory

Evan Bredeweg, Ivan Arismendi and Sarah Henkel
Oregon State University

Alex Cagle, Bella Alvarado, and Alex Meyer
Noria Energy

Dan Berger, Dana Olson, and Daniel Pardo
DNV

Meghan Bringolf, Jose Zayas, and Neal Simmons
Eagle Creek Renewable Energy

Idaho National Laboratory

Battelle Energy Alliance manages INL for the U.S. Department of Energy's Office of Nuclear Energy

INL/RPT-25-
Revision 0

Floating Solar in Hydropower Reservoirs in the United States

Techno-economics, Environmental Considerations, Regulatory Pathways, and Technical Potential

Juan Gallego-Calderon, Tyler B. Phillips, Mucun Sun, and Tanveer Hussain
Idaho National Laboratory
Aaron Levine, Evan Rosenlib, and Marie Rivers
National Renewable Energy Laboratory
Evan Bredeweg, Ivan Arismendi and Sarah Henkel
Oregon State University
Alex Cagle, Bella Alvarado, and Alex Meyer
Noria Energy
Dan Berger, Dana Olson, and Daniel Pardo
DNV
Meghan Bringolf, Jose Zayas, and Neal Simmons
Eagle Creek Renewable Energy

January 202

Idaho National Laboratory
Energy and Water Systems
Idaho Falls, Idaho 83415

http://www.inl.gov

Prepared for the
U.S. Department of Energy
Office of Energy Efficiency and Renewable Energy
Under DOE Idaho Operations Office
Contract DE-AC07-05ID14517

Page intentionally left blank

EXECUTIVE SUMMARY

Overview

The U.S. is rich in energy resources, ranging from fossil fuels to abundant opportunities for alternative energy. The demand for electricity in the U.S. had remained relatively constant since 2007, but that is now changing with the rise of big data centers and the growing need for charging electric cars. Furthermore, the increasing energy demand is forecast to persist through 2050. Because of this, there is a pressing need to develop innovative solutions that are reliable and cost-effective. Floating solar, when coupled with existing reservoirs, presents a unique opportunity to use current infrastructure, such as dams, hydropower facilities, substations, and service roads, potentially removing barriers for development. However, FPV technology remains nascent in the U.S., primarily limited to small man-made water bodies and behind-the-meter applications. Significant questions remain regarding its utility-scale development and the mechanisms needed to make it cost effective.

This report presents a comprehensive analysis of the feasibility of floating photovoltaics (FPV) in federally regulated reservoirs within the continental United States (CONUS) and to present a methodology for capturing the true costs of deployment, potential environmental impacts, and regulatory pathways for open-loop hydropower reservoirs. It is intended for stakeholders who may not be solar industry experts but who are interested in exploring the potential for FPV in their reservoirs. While there are promising opportunities, particularly in enhancing dissolved oxygen (DO) levels and potentially improving compliance with existing hydropower licenses, the current capital costs of FPV are not yet competitive with traditional land-based solar installations at the utility-scale when comparing the LCOE results. A competitive financial outlook is achievable when applying a 30% Investment Tax Credit (ITC)[a] and considering a 5% reduction from the baseline capital expenditures (CapEx) at the Tuckertown Reservoir in North Carolina case study. The study is structured around three key pillars of research: technical potential, environmental impacts and regulatory considerations, and technoeconomic analysis. This report provides a nationwide assessment of the opportunities for FPV in terms of capacity, measured in direct current megawatts (MW_{DC}), in reservoirs managed by the U.S. Bureau of Reclamation (USBR), the U.S. Army Corps of Engineers (USACE), and the Federal Energy Regulatory Commission (FERC). Additionally, the report introduces a heuristic model for estimating the CapEx of utility-scale FPV projects (1–100 MW), offering a baseline cost estimate for stakeholders. Finally, the report applies these models to a case study of a hydropower reservoir in North Carolina to present site-specific results.

Key Findings

The main finding of this study is that there is significant potential for co-locating FPV with existing hydropower reservoirs, but the capital costs are not competitive with land-based solar. There is also a lot of site-specific research that needs to be done to assess the environmental impacts of floating solar; however, the estimates in this report indicate that the co-location with hydropower could provide benefits on increasing the DO, and thus, improving hydropower standing in complying with existing licenses and stakeholders. Additional analysis findings of include the following specifics:

[a] Although H.R. 1 (enacted July 2025) shortened the eligibility window for IRA's clean-energy credits—requiring wind and solar projects to begin construction within 12 months of enactment and be completed within four years or, if a project missed the construction start window, be placed in service by 2027—Investment Tax Credit (ITC) and Product Tax Credit (PTC) provisions remain in effect for qualifying technologies for several more years under current Treasury guidance. The deadline for project completion is further extended to ten years for projects on federal lands.

1. **While the technical potential for this case study in North Carolina is up to 609 MW_{DC}, the transmission capacity across several hydropower plants in the that area covers the river system, limiting its maximum capacity to 33 MW_{DC}**. This offers a glimpse to other reservoirs in the technical potential study in which there will be major limitations, not only in transmission capacity, but also related to the intended purpose of such reservoirs.
2. **The affordability of FPV depends significantly on the location due to irradiance and electricity price sensitivities**. The location in North Carolina, which was the subject of this case study, does not seem competitive with land-based solar due to its lower electricity price. Whereas sites within CAISO, a more favorable location (Sun et al 2024), are more competitive. The addition of costs due to floaters and mooring pose an additional cost when compared to land-based. More work is needed to identify the savings of FPV vs land costs.
3. **The ITC incentive proves to be better for FPV than the production tax credit (PTC)[a],** but both have a significant reduction in the LOCE.
4. **Overall, predicted temperature changes due to coverage by FPV in this case study are not likely to represent an impact to fish habitat suitability in this reservoir**. Summer temperatures are predicted to decrease; however, given the overall warm conditions of the lake, the model did not predict any decrease in the warmwater fish habitat in the summer. In fact, warmwater fish habitat was predicted to increase in summer.
5. **Dissolved oxygen maxima were slightly affected but were on the order of less than 1 mg/L with slightly greater**—though still miniscule—declines in winter; dissolved oxygen minima were not affected in summer or winter. The biggest changes observed were in higher average dissolved oxygen in the summer, which again is likely to be a positive outcome for most aquatic species.

Limitations and Future Work

The main limitation of this work is the environmental modeling. While the model is widely used for hydrodynamics and water quality, and has been validated in numerous studies, its validation for large-scale FPV is currently not possible because there is not data available for these systems. Therefore, the analysis covered in this work should be considered preliminary in their demonstrated benefits of co-location. Moreover, the technical potential of the Tuckertown reservoir is limited to the "maximum deployable FPV" based on the environmental constraints described in the methodology section. This indicates that there are other considerations beyond power production, such as transmission capacity, recreation, environmental and historic preservation, community water supply needs, downstream user water needs, and flood control, that were not part of the analysis. Lastly, the CapEx tools heuristics do not include all possible vendors of floats, solar panels, etc., which might generate differences when a project is moving to the engineering and procurement stage. While these are substantial limitations, the methods described and the results presented provide valuable insights into the opportunities for utility-scale deployment of FPV in CONUS. These opportunities translate to potential future work that could include:

1. Improved techno-economic model to include additional incentives, import tariffs, and revenue from potential water savings.
2. A comprehensive analysis on the cost savings of FPV vs land-based PV related to land purchase/lease savings should be conducted.
3. If a site has significant evaporation savings, it would be interesting to explore the regulatory implications surrounding water rights.
4. Additional stakeholder engagement that includes equipment providers to improve the CapEx and OpEx estimates

5. The methods should be expanded to non-Federal reservoirs so there is a complete picture of CONUS. This will entail analyzing other regulatory pathways at the state and municipal level.

CONTENTS

EXECUTIVE SUMMARY v
ACRONYMS xi
1. INTRODUCTION 14
2. METHODS 17
2.1. Floating PV Technical Potential 17
2.2. Environmental Modeling 19
2.2.1. Modeling Approach 21
2.2.2. Modeling Results 23
2.2.3. General Application 26
2.3. Techno-economic Assessment of FPV 27
2.3.1. The FPV CapEx Tool: A Floating Solar Specific Heuristics Tool to Determine the Investments Required for Utility-scale Solar 28
3. CASE STUDY: THE TUCKERTOWN RESERVOIR 32
3.1. Reservoir Considerations 34
3.1.1. System considerations prior to FPV design 35
3.1.2. CO-LOCATED DESIGN: 33 MW 39
3.2. Techno-economic Assessment 41
3.2.1. Regulatory Considerations for Tuckertown 45
3.2.2. Environmental Considerations 46
4. CONCLUSION 55
5. REFERENCES 55

FIGURES

Figure 1. A rendering of an FPV deployment in conjunction with a hydropower reservoir. 15
Figure 2. As of 2023, there are 26 FPV deployments in the United States with a total of 36 MW installed capacity. 16
Figure 3. Technical potential of FPV in CONUS federally regulated reservoirs. 18
Figure 4. Need caption. 18
Figure 5. Graph of percent change in the average surface temperature for reservoirs across different FPV coverages. 24
Figure 6. Graph of the percent change in Schmidt Stability Index, a measure of stratification strength, for reservoirs across different FPV coverages. 24
Figure 7. Graph of the percent change in thermocline depth for reservoirs across different FPV coverages. 25

Figure 8. Graph of the percent change in mean dissolved oxygen for reservoirs across different FPV coverages. 25
Figure 9. Plot of PCA space with PCs 1 and 2 that was developed using the National Renewable Energy Laboratory database of reservoirs suitable for FPV. 26
Figure 10. Plot of PCA space with PCs 1 and 3 that was developed using the National Renewable Energy Laboratory database of reservoirs suitable for FPV. 27
Figure 11. The workflow of the AquaPV toolkit. 28
Figure 12. The workflow inside the TEA tool in AquaPV. 28
Figure 13. Graphical representation of the heuristics in the piers and anchoring category. 31
Figure 14. Workflow of the FPV CapEx tool in AquaPV 32
Figure 15. Restrictive zones along the Tuckertown station and dam. 34
Figure 16. Three topologies of multi-energy systems. 35
Figure 17. Scenario 1: Layout of hydropower plants along the Yadkin River and operated by ECRE. 37
Figure 18. Scenario 2: Capacity share. 38
Figure 19. Scenario 3: The steady-state analysis of the chosen FPV capacity. 38
Figure 20. Scenario 5: When a circuit braker is open between Tuckertown and High Rock to prevent instabilities in the grid due to the high capacity generated in this configuration. 39
Figure 21. The 33 MW FPV system designed by DNV. 40
Figure 22. An example of the configuration and racking in an FPV island. 40
Figure 23. The hourly generation for a typical year at the Tuckertown reservoir. 41
Figure 24. The monthly generation for a typical year at the Tuckertown reservoir. 41
Figure 25. Example price for one day in the summer. 43
Figure 26. Predicted LMP price for the next 30 years. 43
Figure 27. Seasonal price change for all scenarios in the LMP. 44
Figure 28. The NPV for the case study. 45
Figure 29. Graph of percent change in average surface temperature for J. Percy Priest Reservoir, Tennessee, across different FPV coverages. 50
Figure 30. Graph of percent change in thermocline depth for J. Percy Priest Reservoir, Tennessee, across different FPV coverages. 51
Figure 31. Graph of percent change in Schmidt Stability Index, a measure of stratification strength, for J. Percy Priest Reservoir, Tennessee, across different FPV coverages. 51
Figure 32. Graph of percent change in dissolved oxygen for J. Percy Priest Reservoir, Tennessee, across different FPV coverages. 52
Figure 33. Graph of percent change in potential warmwater fish habitat volume for J. Percy Priest Reservoir, Tennessee, across different FPV coverages. 52
Figure 34. Graph of percent change in potential coldwater fish habitat volume for J. Percy Priest Reservoir, Tennessee, across different FPV coverages. 53

Figure 35. Graph of percent change in outflow water temperature (downstream of dam) from J. Percy Priest Reservoir, Tennessee, across different FPV coverages. 53

Figure 36. Graph of percent change in the number of days in a stratified state for J. Percy Priest Reservoir, Tennessee, across different FPV coverages..... 54

Figure 37. Graph of percent change in mean water temperature of a vertical profile for J. Percy Priest Reservoir, Tennessee, across different FPV coverages. 54

TABLES

Table 1. Need caption. ..... **Error! Bookmark not defined.**

Table 2. Need caption. ..... **Error! Bookmark not defined.**

Table 3. Generalized stressor-receptor matrix for FPV on freshwater aquatic systems. 20

Table 4. List of CE-QUAL-W2 reservoirs that were included in this analysis. 21

Table 5. List of quantified variables from CE-QUAL-W2 model iterations of FPV array impacts. 22

Table 6. Parameters that influence the CapEx in a utility-scale FPV project. 29

Table 7. Heuristics for determining the price of anchoring and mooring. 31

Table 8. Heuristics for determining the cost of a new substation. 32

Table 9. The input values specific to the Tuckertown reservoir FPV design. 42

Table 10. Breakdown of the CapEx for Tuckertown. 42

Table 11. TEA results for the 41.2 MW design at Tuckertown. 44

Table 12. Taxa within each of the receptor categories potentially present in Tuckertown Reservoir. 46

Table 13. The change in response variables in J Percy Priest Reservoir, Tennessee, for FPV coverage ranging from 5–40%. 49

Table 14. Maximum, average, and minimum water temperatures and DO concentrations in Tuckertown and High Rock reservoirs during summer (May–September) and winter (November–February) 2006–2022. 50

Page intentionally left blank

ACRONYMS

ATR	Advanced Test Reactor
DOE	U.S. Department of Energy
DOE-ID	U.S. Department of Energy-Idaho Operations Office
INL	Idaho National Laboratory
MFC	Materials and Fuels Complex
R&D	research and development
FPV	floating photovoltaics
MW	Mega-watt
SAV	submerged aquatic vegetation

Page intentionally left blank

Floating Solar in Hydropower Reservoirs in the United States

Techno-economics, Environmental Considerations, Regulatory Pathways, and Technical Potential

1. INTRODUCTION

Floating solar photovoltaics (FPV) represent a significant advancement in the integrated energy sector, primarily due to their ability to mitigate land scarcity issues while enhancing the efficiency of solar energy generation. The literature highlights the multifaceted benefits of FPV technologies, their adaptability to variable geographic conditions, and the economic advantages they present amidst rising land costs.

Previous research highlights the technical potential of FPV systems across diverse areas in the world. For instance, Rai et al. emphasize Nepal's capacity to integrate FPV systems with existing hydropower facilities, noting high potential due to significant water bodies available for FPV installations (Rai et al. 2020). This assertion aligns with findings from Goswami et al., who explore the benefits of FPV technology in terms of electricity generation over water bodies, highlighting its ability to address land scarcity and enhance project feasibility (Goswami et al. 2019). These studies collectively indicate that the adaptability of FPV systems enables optimized energy generation while preserving land resources.

In some cases, FPV systems outperform traditional land-based solar installations. The cooling effect provided by water has emerged as a critical factor for enhancing not only the efficiency but also the energy output of FPV systems. Fadliondi et al. demonstrate that FPV plants can achieve superior power outputs due to the cooling effects from the water (Fadliondi et al. 2023). Supporting insights from Wu et al. further confirm that FPV systems generally produce more energy than terrestrial counterparts due to the benefits of cooling (Wu et al. 2024). Additionally, Yang et al. reveal that FPV systems can positively influence local ecosystems by inhibiting harmful algae growth, thus contributing to improved water quality (Yang et al. 2022).

FPVs exhibit considerable economic potential, particularly in regions where land availability is constrained. A systematic analysis of levelized costs of electricity (LCOE) reveals that FPV installations in Indonesia can often achieve costs as low as $0.1/kWh when incorporated with battery energy storage systems (BESS), which significantly undercuts diesel generators that dominate off-grid operations with LCOEs of $0.3/kWh to $0.5/kWh (Esparza et al. 2024). This cost advantage is crucial for island communities and remote areas heavily reliant on fossil fuel imports. Furthermore, substantial savings can be realized in terms of land and water management; a techno-economic feasibility study indicated that FPV systems could produce 10.2% more generating capacity than traditional land-based installations, translating into significant financial returns over the life cycle of the plant (Goswami et al. 2019). However, the capital costs values used in the previous work seem optimistic with respect to the current state of affairs in the U.S.

In addition to LCOE assessments, various studies have employed net present value (NPV) analyses to highlight the long-term financial benefits of FPV technologies. Mumtaz et al. conducted a comprehensive assessment across diverse climatic zones, demonstrating that the NPV for FPV plants can surpass that of traditional systems when considering site-specific conditions (Mumtaz et al. 2024). Economic analyses further reveal that FPV systems can yield favorable returns, especially when cooling effects from water bodies are factored into operational efficiency (Sukarso and Kim 2020). This cooling mechanism not only enhances energy output but also extends system lifespans, thereby increasing overall investment returns. Additionally, reports indicate that the initial capital investment for FPV systems may be higher than that for land-based installations; nonetheless, the reduced land-use costs and increased generating capacity offset this disparity (Deilami et al. 2024). For example, while FPV installations may incur approximately 20% higher initial costs, they consistently demonstrate enhanced efficiency—averaging 2.54% higher than ground-mounted systems—due to the favorable thermal conditions provided by water bodies (Deilami et al. 2024). As a result, FPV technologies can play a pivotal role in achieving sustainable energy goals, particularly in countries contending with escalating land prices and population densities.

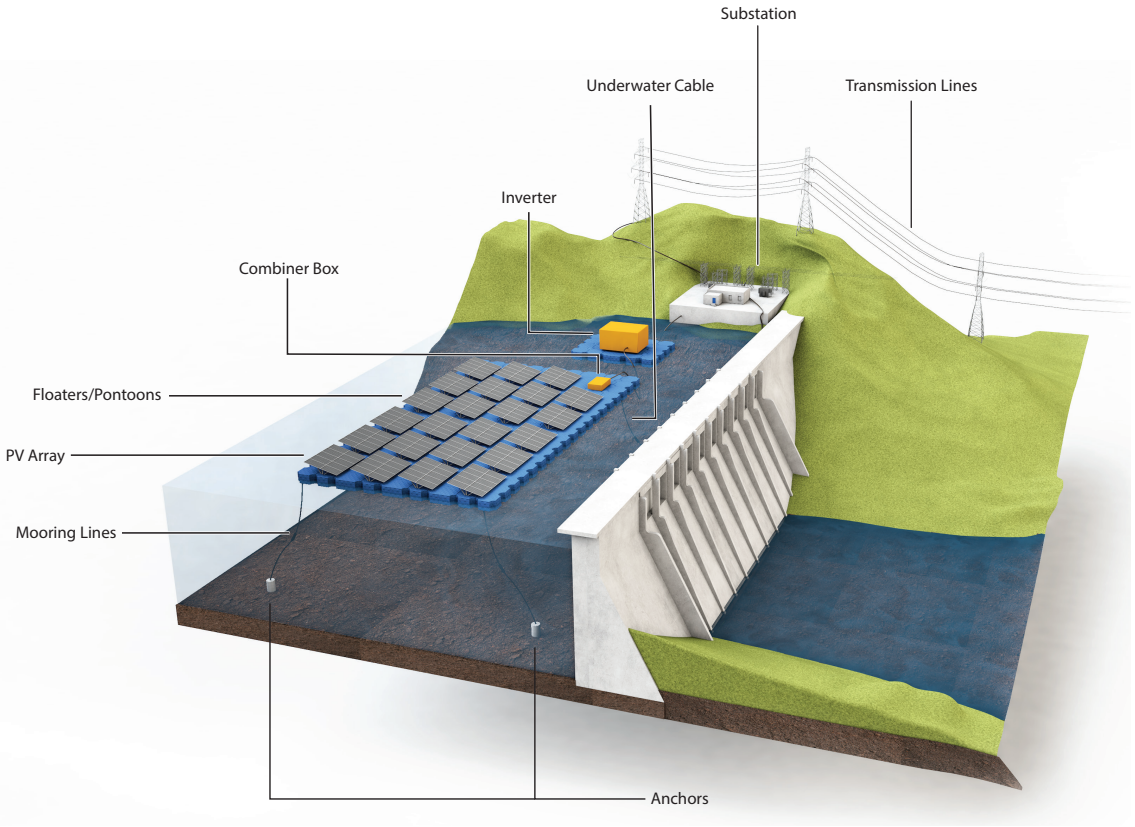

Figure 1. A rendering of an FPV deployment in conjunction with a hydropower reservoir.

The economic landscape for FPV is also accentuated by technology integration with hydroelectric systems. Catania et al. highlighted successful techno-economic assessments showing that integrating FPV with pumped hydro storage not only increases energy generation but also lowers overall system operational costs (Catania et al. 2024). Such synergies illustrate the multifaceted financial benefits of FPV installations in a broader integrated energy framework.

Despite their potential, challenges remain in adopting FPV technologies on a wider scale, particularly in understanding their environmental impacts and technical barriers. Santos-Borja highlights the necessity for further research on the ecological effects of deploying FPV systems in natural water bodies, suggesting that they can offer considerable advantages, provided that local ecosystems are appropriately considered (Rai et al. 2020). Furthermore, Zareef et al. address the technical integration of FPV into existing energy grids, emphasizing the innovative solutions required to overcome these obstacles (Wu et al. 2024).

Despite these advances worldwide, FPV systems are a relatively new approach in energy infrastructure, and as such, the number of arrays deployed in the U.S. has been somewhat limited. To date, the installations of FPV have been primarily located in Florida, California, and New Jersey. While one of the earliest non-research adopters of FPV arrays was the Far Niente Winery, with an installation dated 2008, most installations have been installed after 2018. These installations have been deployed in various contexts that include agricultural irrigation ponds, water treatment reservoirs, and recreation reservoirs. The most common types of water bodies for FPV deployments in the U.S. have been on retention ponds or water treatment facility ponds (n=8 and n=6, respectively). Of the 26 installations recorded as of 2023, only one of these FPV arrays was deployed on a state-owned reservoir (Figure 2). There are no current FPV arrays deployed in conjunction with hydroelectric infrastructure in the USA, nor reservoirs managed by federal agencies.

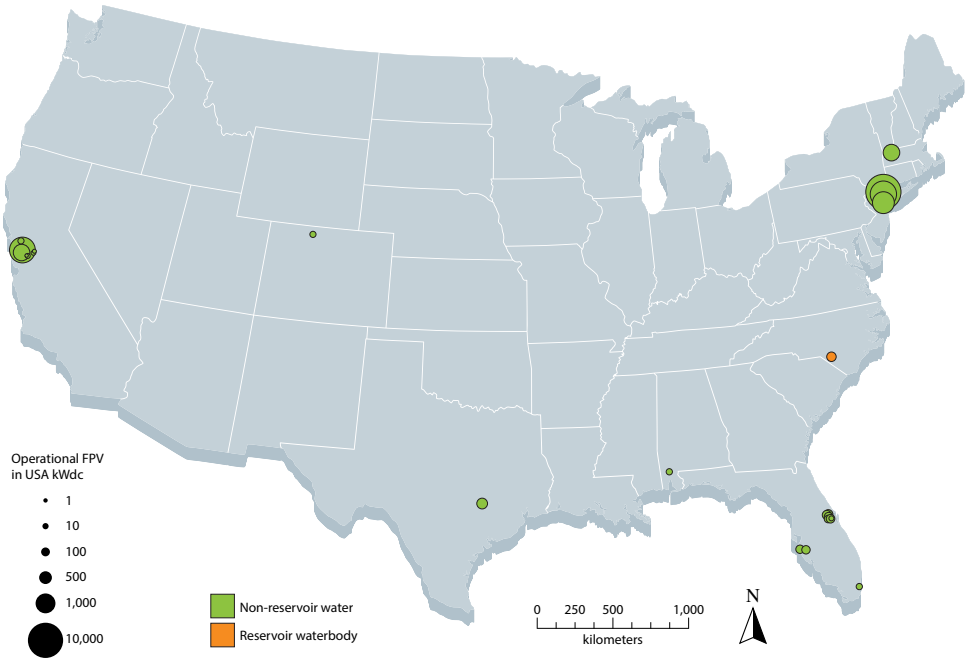

Figure 2. As of 2023, there are 26 FPV deployments in the United States with a total of 36 MW installed capacity.

The scale of the deployments in the U.S. has also varied. The average energy generation of a U.S.-based FPV array was 1,397 kWdc[b]. The smallest installation was a research array deployed by UC Davis (1 kWdc), while the largest FPV array is located at the Canoe Brook Water Treatment Plant (8,900 kWdc). The only reservoir-based floating PV was an array of 1,100 kWdc, which was installed in 2022 on Big Muddy Lake located south of Camp Mackall in Fort Bragg, North Carolina (U.S. Army Public Affairs 2022). The total FPV generation capacity of all USA arrays is around 36 MWdc, which is a small proportion of the 2021 globally installed 3,800 MWdc cumulative capacity (Silalahi and Blakers 2023). Much of the current global capacity exists in Asia, with China, Japan, and Korea dominating installed FPV capacity (Ma, Wu, and Su 2021). While FPV is a new application type for solar installations, the pace of FPV deployments in the United States has been slower than in other countries. This bias has also been reflected in the published literature researching the ecological impacts of FPV arrays. A review from 2023 cataloged 25 publications researching ecological effects of FPV using empirical and modeling approaches with no publication based out of the USA (Nobre et al. 2023).

FPV has the potential to increase overall energy production from existing hydropower reservoirs. This technical report delves into a comprehensive techno-economic analysis (TEA) and environmental considerations associated with deploying FPV in hydropower reservoirs. It highlights the technical potential of federally regulated reservoirs and draws upon case studies and empirical data to furnish an in-depth overview of the current state of FPV technology. By examining the successes and challenges faced by existing installations, the report elucidates the scalability of FPV systems and their potential role in a future energy system.

2. METHODS

2.1. Floating PV Technical Potential

The United States' technical resource potential analysis for FPV on federally owned or licensed reservoirs estimated the potential area, PV capacity, and average expected generation that is technically feasible to develop. This analysis focused on reservoirs owned by the U.S. Army Corps of Engineers (USACE), the U.S. Bureau of Reclamation (USBR), and those associated with a Federal Energy Regulatory Commission (FERC) licensed hydropower dam. Initially, reservoirs in these categories were filtered to exclude those completely infeasible for FPV development. Subsequently, geospatial methods were used to model the available surface area available for FPV development on each remaining reservoir. The two criteria that exclude a reservoir from FPV entirely are (1) being part of a USACE-maintained navigable waterway, which would subject any FPV development to large freight shipping wakes or (2) being in climates with extreme winter weather, which subjects FPV to excessive snow loading and the potential for ice flows.

The remaining technical exclusion criteria exclude areas within the water body that are not likely to be developable for FPV. These reductions in the developable area of a reservoir primarily come from the following:

1. Exclusion buffers from hydrological inlets and outlets, scaled as a function of peak monthly flow rate, due to the potential for swift currents in hydrological forebay and tailrace zones
2. Safety and maintenance exclusion buffers from dams of 100 meters
3. Areas that are likely to be both dry at low reservoir fill levels and that are not flat enough to support the grounding of FPV floats.

[b] kWdc is the analogous to the installed capacity based on the DC value of the panels. For example, 3 panels of 600 W, will yield 1,800 Wdc. However, the conversion to AC yields a different value and depends on the inverter, system efficiency, etc

Multiple values for minimum fill volumes and maximum reservoir floor slopes were considered to quantify the results sensitivity to estimate parameters. Maximum average floor slopes of 2% and 3% were used to determine whether the floor was flat enough to design FPV floats to be grounded at low fill volumes. Low fill-level volumes of 25% and 35% were used to model reservoir surface areas at low fill levels. These minimum fill values were chosen to conservatively represent the lower end of common fill volumes for all reservoirs in the continental United States. Particularly in the arid western contiguous United States, reservoirs typically have wide seasonal variation in their water elevations due to the highly seasonal nature of inflows (typically driven by spring runoff) and water demand (typically driven by high summer agricultural irrigation use for reservoirs that are used for that purpose in addition to hydropower generation).

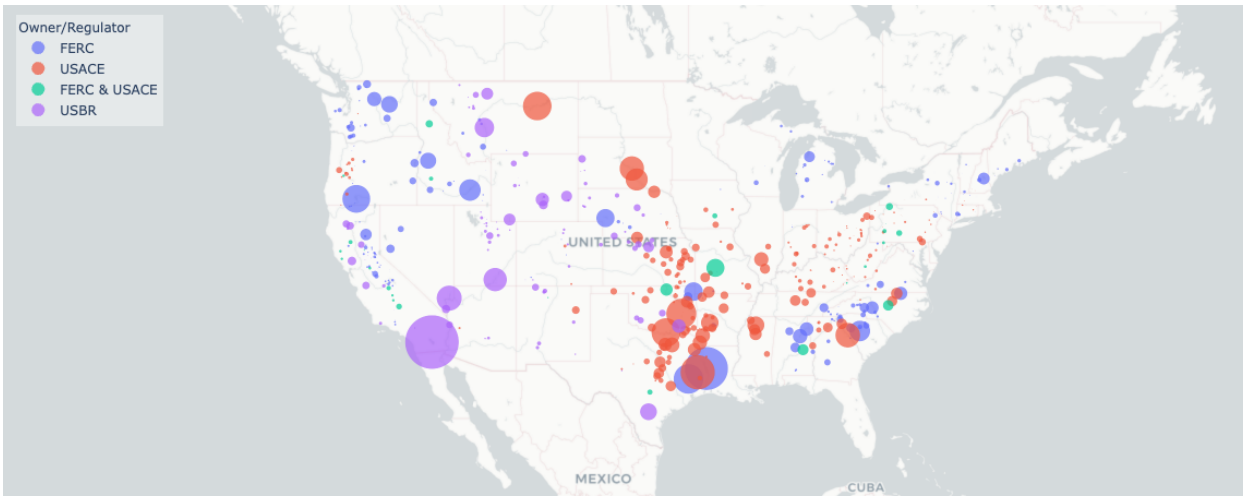

Figure 3. Technical potential of FPV in CONUS federally regulated reservoirs.

To estimate the developable area for FPV, each exclusion zone is subtracted from the reservoir polygon, and the area of the remaining polygon is recalculated. The FPV capacity in nameplate DC megawatts is calculated from the available area assuming a conversion ratio of 1 MW_{DC} per hectare of available surface area. Average annual generation for this associated capacity is estimated using the PvWatts application programming interface (API) to predict the performance of a fixed tilt PV system with the low panel tilt of 12 degrees typical of FPV installations (Dobos 2014). FPV generation results are increased by 3% to account for the efficiency gains resulting from the cooling effect of water on PV panels.

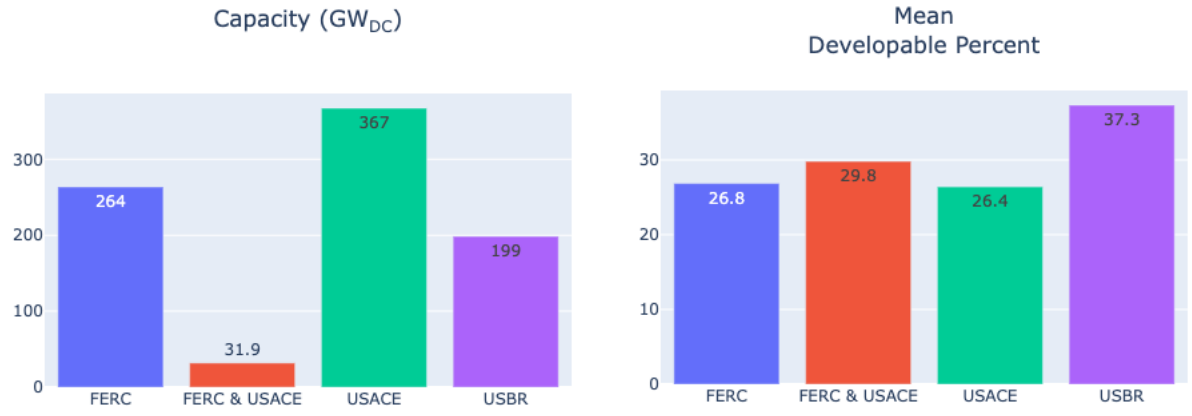

Figure 4. Distribution between the type of reservoirs of capacity and the FPV developable percent.

2.2. Environmental Modeling

The range of potential deployment locations of FPV systems has been a key feature discussed in the development of this technology. This does create complexity when assessing potential environmental impacts as different aquatic environments have unique ecologies and tolerances to changing conditions. A stressor-receptor approach, based on a U.S. Environmental Protection Agency framework for ecological risk (EPA 1998), has frequently been used to consider potential effects of offshore energy sources, such as wave, tidal, or wind (e.g., McMurray 2008, Boehlert and Gill 2010, Copping et al. 2011, Henkel et al. 2013), and can be useful for this integrated energy application. Generic components of FPV installations that may have environmental effects (stressors) are the floating components: the panels themselves and any other equipment that may be located on floats, including inverters, transformers, or various combiner boxes; water column-spanning components of the mooring system; and anchors if the project is not entirely shore-moored. Some interactions of concern may be short term (e.g., during construction or decommissioning), while others will persist for the duration of operations. Generic receptors are habitats and/or biota present in the system that may be affected by each of the project components. The interaction of stressors (i.e., those parts of a project that may cause changes to the environment) and the receptors (i.e., habitat features, organismal groups) can be used to identify potential environmental issues of concern. Once these general interactions have been identified, a site/project specific investigation is needed to determine what local habitats/biota are present and likely to be susceptible to the effects of project components and subsequent environmental changes.

The potential ecological impacts of FPV on freshwater (Exley et al. 2021b, Nobre et al. 2023) as well as coastal and marine (Benjamins et al. 2024) systems have been thoroughly reviewed. These reviews form the basis for the generic stressor-receptor table presented here (Table 1), where the highlighted cells represent expected interactions between some project component or physical changes associated with it and a biological receptor. The shielding aspects of the floating components may result in reduced irradiation and reduced wind (stressors), which will have effects on water-atmosphere interchange, water temperature, evaporation, mixing/stratification, and, potentially, oxygen, nutrient, and salinity gradients. These potential water property changes can affect all species in the aquatic system. Reduced irradiation can have direct effects on autotrophs (e.g., phytoplankton and blue-green algae in the water column as well as and bottom-associated plants, algae, and flagellates) along with zooplankton, fishes, and invertebrates that undergo vertical migrations triggered by light. Changes to phytoplankton can have cascading trophic effects on zooplankton and fishes while changes to submerged aquatic vegetation (SAV) may have trophic impacts on herbivorous fishes and turtles. The actual structures on the surface can reduce bird foraging directly under the panels but may provide opportunity for increased bird roosting and nesting if there is space between the PV panels and the support structures. This increased presence of birds in the vicinity of the panels could increase foraging in areas around the panels and result in pulses of nutrient input as bird droppings get flushed into the water during rainfall or cleaning events. The panels may attract polarotactic (attracted to water-reflected light) insects, which can affect the reproductive success of these insects and also reduce opportunities for foraging on these insects and/or their eggs by surface-feeding fishes. The undersides of surface components as well as water column-spanning components of the mooring system and anchors can be colonized by fouling biota, and the installation of the anchors can disturb bottom-associated biota. Noise, primarily during installation, is likely to affect birds as well as fish and aquatic invertebrates, although any disturbance will be temporary.

Table 1. Generalized stressor-receptor matrix for FPV on freshwater aquatic systems.

	Reduced light	Reduced wind	Structure on surface	Structure in water column (e.g., mooring lines)	Structure on bottom (e.g., anchors)	Acoustic effects (primarily during installation)
Temperature	■	■				
Dissolved oxygen	■	■				
Phytoplankton	■	■				
Native SAV	■	■			■	
Noxious SAV	■	■			■	
Blue-green algae	■	■			■	
Sediment-inhabiting flagellates	■				■	
Native FW mussels	■	■			■	
Invasive invertebrates	■	■			■	
Other invertebrates	■	■			■	■
Fish	■	■	■	■	■	■
Zooplankton	■	■				
Turtles	■	■				■
Fouling biota			■	■	■	
Insects			■			
Birds			■			■

The installation of large-scale FPV on freshwater bodies has the potential to influence the thermodynamics, food webs, and other processes of the aquatic ecosystem. The primary mechanisms identified by which FPV can impact reservoirs are changing incoming solar radiation (i.e., shading) and modifications to the water-air boundary interactions (i.e. wind sheltering). These factors can change the water temperature, mixing, and ultimately thermal stratification. This is key in freshwater systems, as the water temperature determines the rates of other chemical processes and the context for a host of biological processes.

With the growing interest in adding to the U.S. energy portfolio, it is important to broadly determine the potential impacts of FPV arrays on existing ecosystems in federally-managed reservoirs in the U.S. so that authorities and policy-makers can plan and manage for impacts on important species. To accomplish this, mechanistic models of freshwater reservoirs were used to create informed predictions of physical responses to various FPV array sizes, which could have ecological consequences. These mechanistic models enable controlled changes to some aspects of reservoir processes while measuring the responses within the water body. While floating PV systems on natural lakes do share many factors with the

ecological impacts that may be experienced in reservoirs, their differences in physical form (specifically, variation in depth along the length of the water body) would require a different strategy to assess response variables.

2.2.1. Modeling Approach

This analysis used the CE-QUAL-W2 mechanistic modeling software. CE-QUAL-W2 is a laterally-averaged quasi-2D hydrodynamic and water quality model that has been widely used to model various freshwater systems. In particular, this model was selected because of the history of model development for hydroelectric reservoirs. The analysis includes 11 different reservoirs that had climate and hydrological data fit to CE-QUAL-W2 models (Table 2). The analysis of water body responses was executed by varying the shade and wind sheltering variables for areas of surface water under FPV arrays. To assess the potential impact of FPV, nine response variables (Table 3) were tracked for a model year with various FPV array sizes or coverage percentages, as described below. The modeled year varied by reservoir as each of the reservoirs had different available climate and hydrological data. To compare model responses across reservoirs, modeled response variables are plotted as percent change relative to reference conditions (without modification to shade and wind sheltering) rather than absolute change. For those reservoirs for which multiple years of data are available (or if measurements are made in future years), the models could be run for multiple years and interannual comparisons of responses could be made.

Table 2. List of CE-QUAL-W2 reservoirs that were included in this analysis.

Reservoir	State	Area (km2)	Depth (m)	Dissolved O2	Retention Time (days)
Foster Reservoir	Oregon	3.64	30.78		7.5
Berlin Lake	Ohio	5.74	16.76	X	46.7
Green Peter Reservoir	Oregon	8.51	96.01		80.8
Milton Lake	Ohio	8.51	10	X	53.9
Detroit Reservoir	Oregon	8.82	95.98		91.7
MJ Kirwan Lake	Ohio	10.1	10.39	X	189.1
Long Lake	Washington	17	54.86		10.9
Mosquito Creek Lake	Ohio	23.1	5.4	X	229.7
Dworshak Pool	Idaho	36.6	198.12	X	151.0
J. Percy Priest Reservoir	Tennessee	46.3	11.73	X	171.9
Degray Reservoir	Arkansas	55.8	61	X	796.7

Because of the unique context of each reservoir, the analysis uses an unmodified model run as a baseline scenario to compare against test model runs to quantify the influence of FPV arrays relative to that reference model. The CE-QUAL-W2 model simplifies the surface of reservoir water bodies into segments that span the shore-to-shore width along the length of the waterway. These segments can have independent variables dictating shade and wind sheltering for that specific segment area. By adjusting these variables for specific segments, it is possible to localize the floating PV array within the model framework. FPV arrays were assumed to be installed on downstream areas of reservoirs (closest to hydroelectric infrastructure) with increasing floating PV arrays extending in the reservoir upstream. For each test model run, modifications were made to shade or wind-sheltering variables on specific segments of the reservoir that related to the FPV array size. First, the lowest level of the reservoir within the baseline model run was identified, and the level was used to calculate the reservoir area at the lowest water level. This minimum area value was then used to determine the steps in the model iterations. Models were run iteratively with an increasing FPV area, which increased by 0.5 square kilometers (50 hectares) or 5% of the minimum reservoir area, whichever was less. These iteration array sizes were then used to partially or fully cover specific water segments working upstream in the reservoir until the associated array size was reached.

This report uses the assumption that FPV arrays directly reduce incoming sunlight and water-air interactions at a fixed rate of 1:1. For example, two segments with 100% and 50% coverage, respectively, would have an effective reduction of sunlight of 100% and 50% and wind-sheltering of 100% and 50%. The nature of these relationships between shading, wind, and FPV array represent the most impactful scenario, and in reality, the nature of light and wind interaction will be dependent on the specifics of the mounting panels system. For example, studies have found that different PV mounting systems change the environment directly beneath the panels differently (Bax et al. 2023). Another simulation of FPV arrays with direct measurements of a system estimated that FPV arrays reduced sunlight by 73% and wind speed by 23% for the covered area (Ilgen et al. 2023). As the reduction of sunlight and wind will depend on the characteristics of the installed system as well as the angle of incoming radiation (latitude- and season-dependent) this study maintained the assumed 1:1 relationship for comparisons of all the reservoirs, the exact nature of effects from FPV arrays should account for differential levels of shading and wind sheltering that various mounting systems create.

Each of these model iterations were run sequentially with key measurements of the reservoir recorded. Response variables for each model iteration were extracted for winter (Jan–Feb) and summer (July–Aug) seasons and scaled to percent change from the reference baseline model. The data from each model iteration was compiled into a database to use in the AquaPV webtool.

Table 3. List of quantified variables from CE-QUAL-W2 model iterations of FPV array impacts.

Variable	Location
Schmidt Stability Index	Outflow
Vertical Profile Temperature	Outflow
Vertical Profile Dissolved Oxygen (when present)	Outflow
Number of Stratified Days in Seasonal Window	Outflow
Depth of Thermocline	Outflow
Surface Water Temperature	Full reservoir
Outflow Temperature	Outflow
Warmwater Fish Habitat (when dissolved oxygen is present)	Full reservoir
Coldwater Fish Habitat (when dissolved oxygen is present)	Full reservoir

2.2.2. Modeling Results

The impact of simulated FPV arrays on response variables had generalizable trends; however, some water bodies had markedly different response trends from most reservoirs. Increased covered surface resulted in decreasing surface temperatures for all modeled reservoirs; however, some water bodies exhibited greater percentage declines in summer months, while others had the greatest modeled changes in winter (Figure 5). In a review of ecological impacts of FPV systems, this trend of a decreasing surface temperature was reported in 55% (11/20) of studies (Liu et al. 2023).

Schmidt Stability, a measure of the strength of thermal stratification, was generally consistent during summer months regardless of the percent coverage, but it increased with FPV coverage during winter months with great variability among reservoirs in the magnitude of the percent change (Figure 6). This increasing strength of stratification changed some reservoirs from a monomictic (stratified only once per year) to a dimictic (stratified twice per year) state. The thermocline depth also had a non-linear response for each season: Summer thermoclines were deeper at lower PV coverage and then became shallower at high percent coverage; winter thermoclines became shallower until they reached a steady threshold (Figure 7). These non-linear relationships mirrored other simulations of FPV arrays, which also found that these response variables were particularly sensitive to the values of shade and wind sheltering that the array design created (Exley et al. 2021a; Ilgen et al. 2023).

The response of DO was one of the most variable between reservoirs with general higher values relative to the baseline in summer months and a negative trend with increasing coverage in winter months; although, values varied little from the baseline for all but one reservoir (Figure 8). DO was reported to decrease in 45% (9/20) of the studies in a review (Liu et al. 2023), but modeling work by Yang et al. (2022) found that the changes in DO were potentially localized around arrays, which could explain the discrepancy with this report's response variable at consistent downstream segments. This form of modeled response tracks these changes in the reservoir as a unit, which does limit the comparison with research that compares areas underneath and apart from FPV arrays (de Lima et al. 2021; Bax et al. 2023; Liu et al. 2023; Atikah et al. 2024; Ziar et al. 2021). The localized effects of FPV arrays compared to reference locations within a single water body may be distinct from systemic changes to the full water body (e.g., duration of stratification, depth of thermocline, mean surface temperature) as modeled using CE-QUAL-W2.

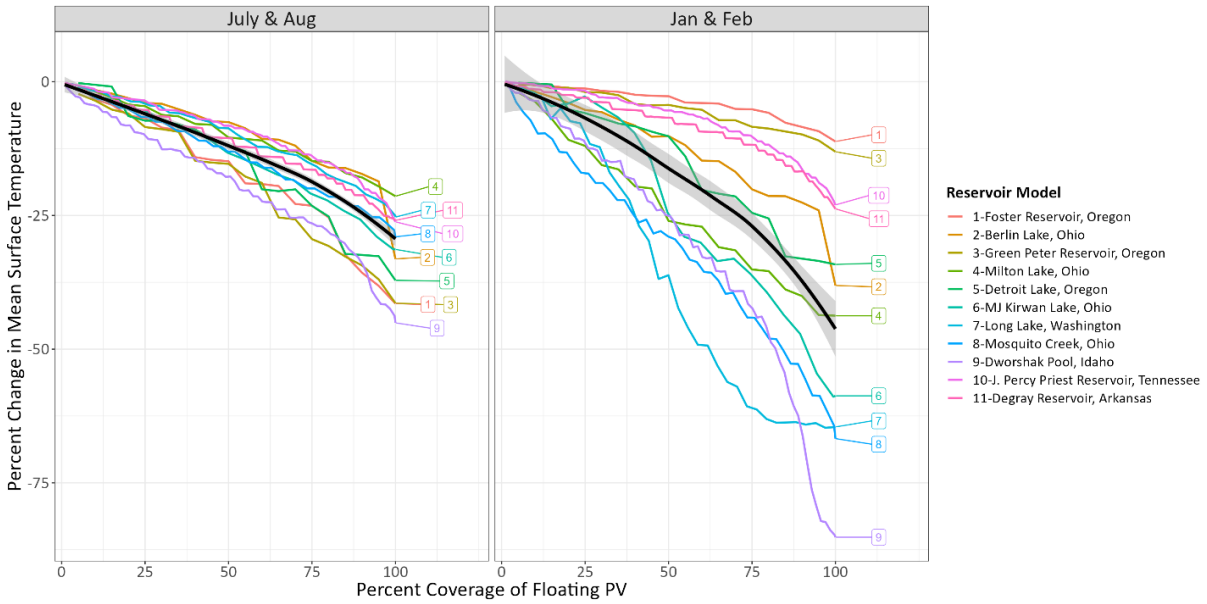

Figure 5. Graph of percent change in the average surface temperature for reservoirs across different FPV coverages. Summer months of July and August are separated from winter months of January and February. Reservoirs are sorted from smallest to largest. The black trend line represents the loess regression with grey standard error.

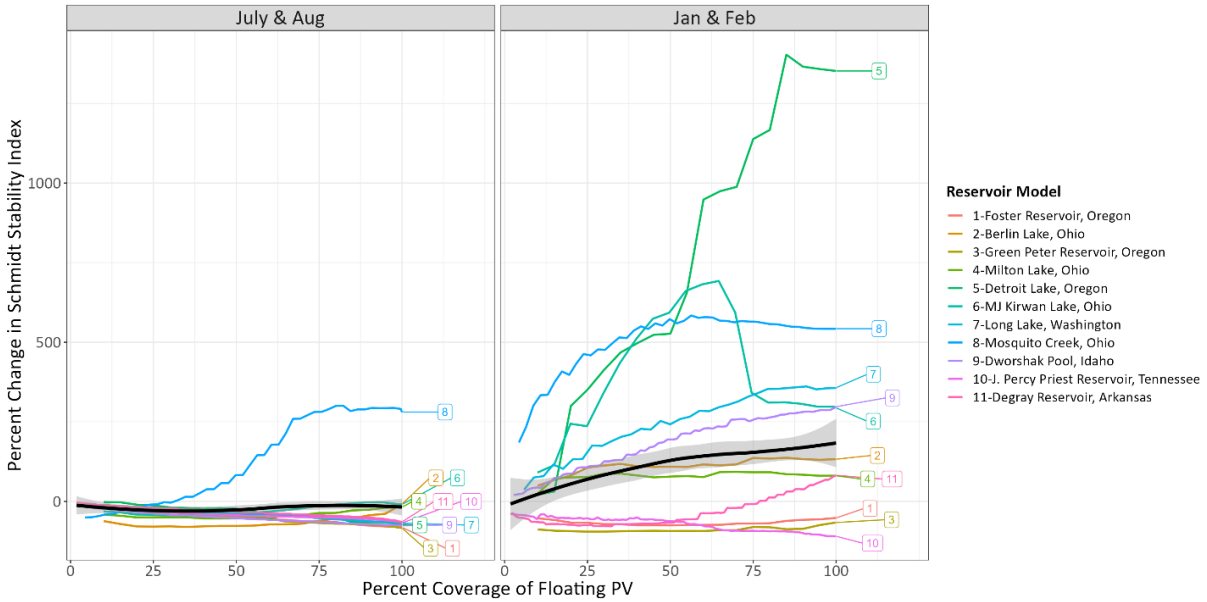

Figure 6. Graph of the percent change in Schmidt Stability Index, a measure of stratification strength, for reservoirs across different FPV coverages. Summer months of July and August are separated from winter months of January and February. Reservoirs are sorted from smallest to largest. The black trend line represents the loess regression with grey standard error.

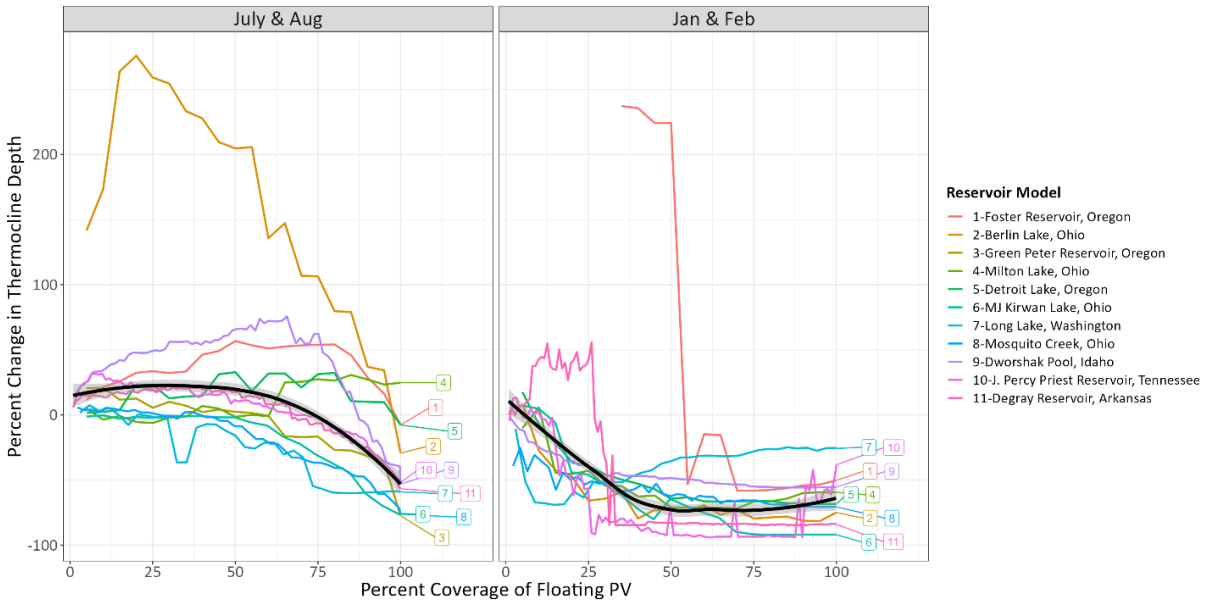

Figure 7. Graph of the percent change in thermocline depth for reservoirs across different FPV coverages. Summer months of July and August are separated from winter months of January and February. Reservoirs are sorted from smallest to largest. The black trend line represents the loess regression with grey standard error.

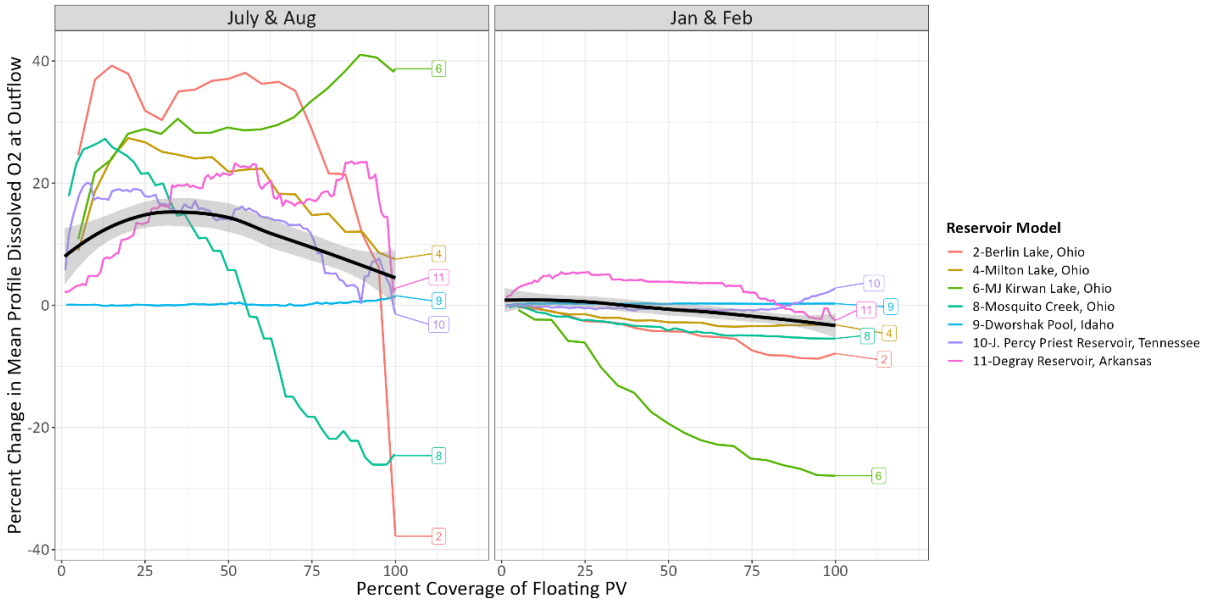

Figure 8. Graph of the percent change in mean dissolved oxygen for reservoirs across different FPV coverages. The average is taken from the vertical profile of the most downstream segment from reservoir model. Summer months of July and August are separated from winter months of January and February. Reservoirs are sorted from smallest to largest. The black trend line represents the loess regression with grey standard error.

2.2.3. General Application

The 11 model reservoirs were used as a population of potential response relationships. To understand how a particular candidate FPV site might respond to panel coverage , a principal component analysis (PCA) was performed on reservoir characteristics (e.g., depth, area, elevation, latitude, longitude, drainage area, shoreline development index) and bioclimatic variables (see WorldClim, Fick and Hijmans 2017). Only s variables that were correlated to other variables at a rate of less than 0.9 were included in the PCA. The resulting PCAs (Figure 9 and Figure 10) provide a distance relationship that combines variability across the reservoir characteristics to estimate physical similarity between individual water bodies. The distances were calculated from each potential FPV site to each of the 11 model reservoirs and are available in the AquaPV Toolkit. The modeled reservoir with the smallest distance in this PCA space from the candidate, unmodeled reservoir can then be considered as a proxy for potential environmental responses to different FPV array coverages.

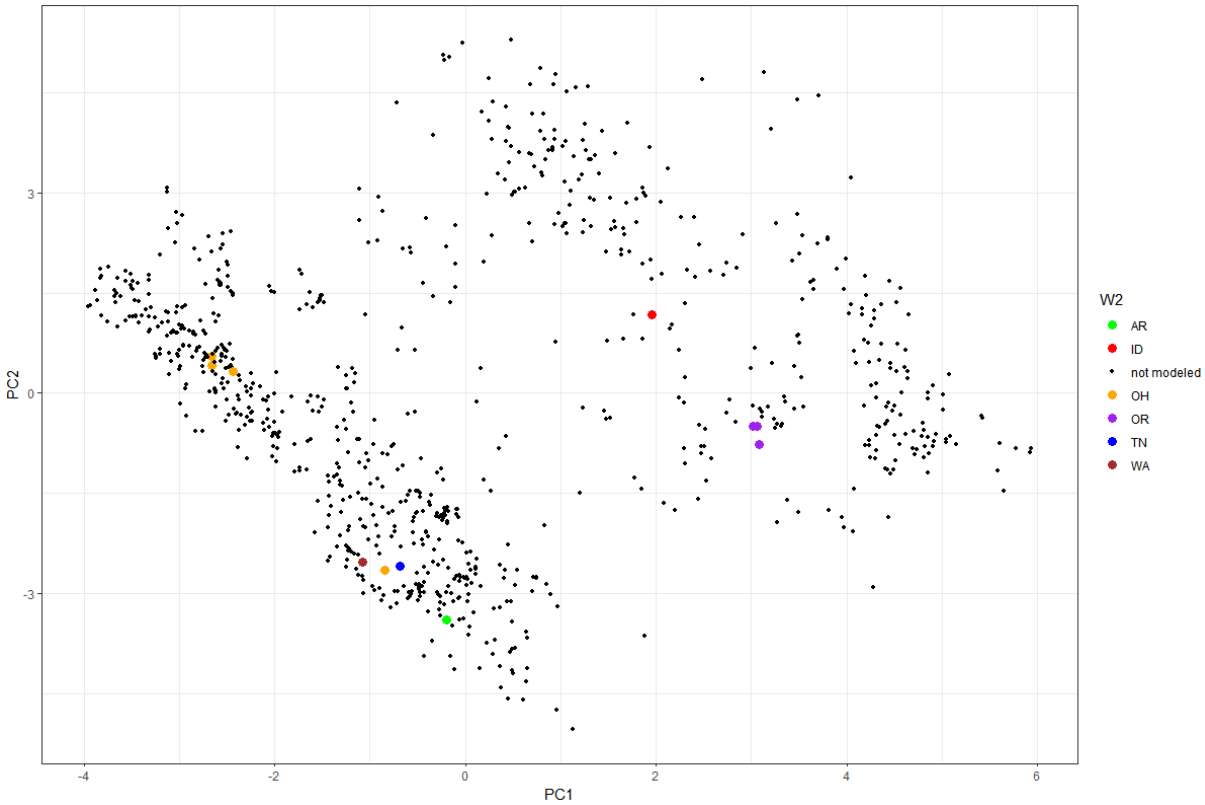

Figure 9. Plot of PCA space with PCs 1 and 2 that was developed using the National Renewable Energy Laboratory database of reservoirs suitable for FPV. Variables used in the analysis included depth, area, elevation, latitude, longitude, drainage area, shoreline development index, and WorldClim bioclimatic variables that were not highly correlated with other variables (excluded after r=0.9). Reservoirs simulated with CE-QUAL-W2 are shown in the color indicating which state they are located in. Non-modeled reservoirs are shown in black.

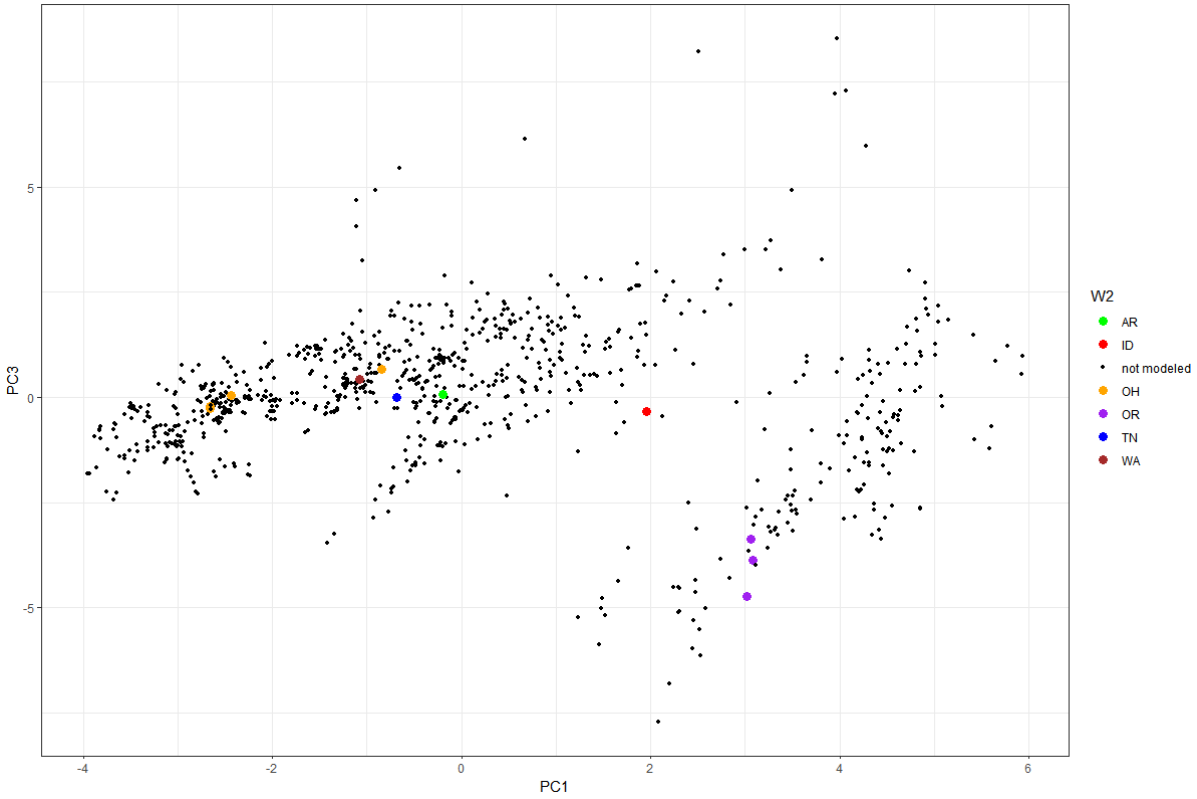

Figure 10. Plot of PCA space with PCs 1 and 3 that was developed using the National Renewable Energy Laboratory database of reservoirs suitable for FPV. Variables used in the analysis included depth, area, elevation, latitude, longitude, drainage area, shoreline development index, and WorldClim bioclimatic variables that were not highly correlated with other variables (excluded after r=0.9). Reservoirs simulated with CE-QUAL-W2 are shown in the color indicating which state they are located in. Non-modeled reservoirs are shown in black.

2.3. Techno-economic Assessment of FPV

The techno-economic analysis (TEA) of utility-scale FPV involves evaluating both the technological feasibility and economic viability on a site-specific basis. This analysis is crucial for stakeholders, including hydropower and solar power developers, policymakers, investors, and utilities, as it provides a comprehensive understanding of the costs, benefits, and potential challenges associated with deploying FPV on a utility scale.

Utility-scale FPV refers to large solar installations in water bodies that are designed to supply electricity to the bulk power system, typically producing energy in the range of tens to hundreds of megawatts. The analysis involves various factors, such as determining the capital expenditures (CapEx), operational expenditures (OpEx), levelized cost of electricity (LCOE), NPV, return on investment (ROI), and the potential environmental impacts. It also considers the integration of solar power into the existing grid infrastructure, which includes assessing available substation capacity, transmission capacity, storage needs, grid stability, and the impacts of intermittent energy production.

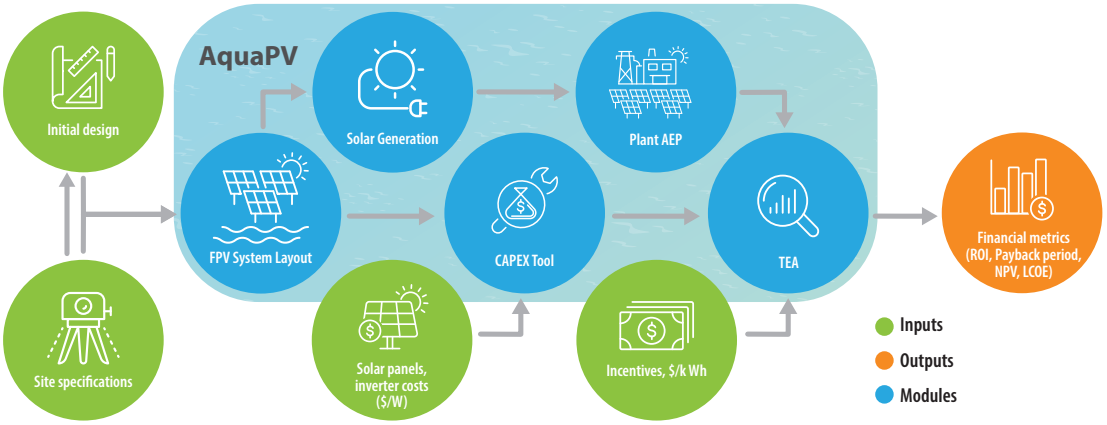

Figure 11. The workflow of the AquaPV toolkit.

The AquaPV toolkit (Figure 11) was developed to support stakeholders in the pre-feasibility stages of a utility-scale FPV with several tools to carry out a TEA (Figure 12). As with any TEA exercise, the workflow starts with a set of site specifications such as system size (MW_{DC}), location, distance to shore, local and federal incentives, and CapEx and OpEx. Specific to the FPV system layout, the user inputs other system efficiency considerations such as DC to alternating current (AC) ratio, system efficiency, and tilt angle. These are used to compute the solar generation time series and plant annual energy production specific to the location.

In recent years, the declining costs of solar technology and advancements in energy storage have made utility-scale solar an increasingly competitive option compared to traditional fossil fuels and other energy sources. However, in the case of FPV in the U.S., the economic feasibility of these projects still depends heavily on geographic location, supply chain constraints, pathways to permitting and licensing, policy incentives, and market conditions.

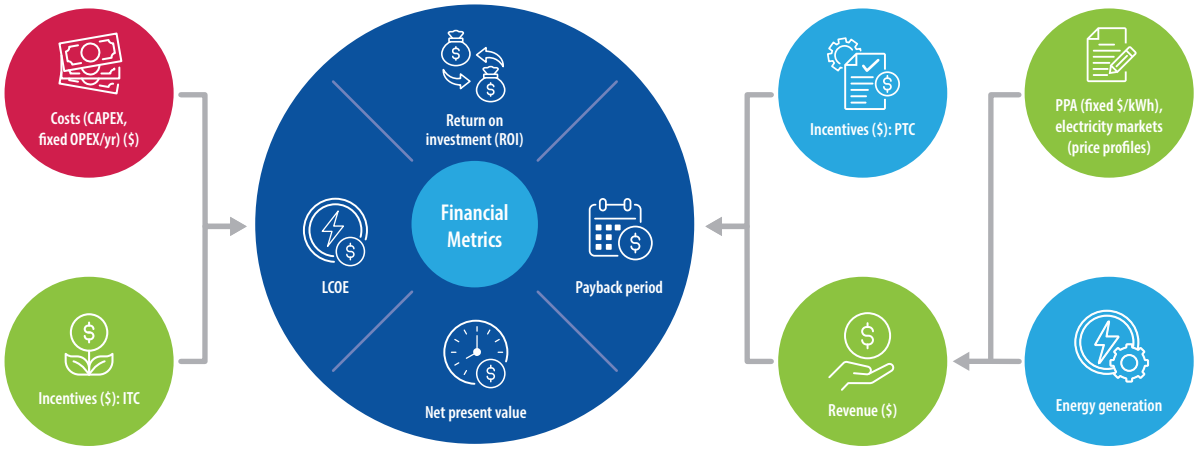

Figure 12. The workflow inside the TEA tool in AquaPV.

2.3.1. The FPV CapEx Tool: A Floating Solar Specific Heuristics Tool to Determine the Investments Required for Utility-scale Solar

To estimate the CapEx for utility-scale FPV projects, a heuristic analysis was used by examining data from currently deployed projects. This approach leverages real-world trends and projects deployed in the U.S. to derive cost estimates that can be applied to similar future projects in the U.S. with capacities ranging from 1–100 MW_{AC}. The components included in the analysis are shown in Table 4.

Table 4. Parameters that influence the CapEx in a utility-scale FPV project.

Hard costs	Solar panels	This category represents the cost of solar PV modules for the project.
	Install labor	This category includes all installation costs associated with the FPV installation. This includes installation for all components across the previous segments and construction of support structures such as concrete equipment pads.
	Racking	The cost of all racking components and racking structures, including floats, panel mounts, and associated racking hardware. This category does not include additional materials outside of the floating structure such as anchor and mooring materials, wiring, or electrical equipment.
	DC EBOS	This category includes all electrical balance of system wiring costs associated with the DC electrical components of the FPV. Specifically, this includes wiring along rows to combiner boxes and combiner boxes to inverters.
	Inverter	This category represents the cost of inverters for the project.
	Anchoring and Mooring	This category includes all material associated with anchors, mooring lines, and related materials. This category does not include installation cost for anchor/mooring, or the associated machinery needed for anchor deployment (e.g., barges, divers).
	AC EBOS	This category includes all electrical balance of system components on the AC portion of the FPV installation. Specifically, this includes wiring from inverter to transformer.
	Gen-Tie	The gen-tie category includes all wiring/tie-in equipment from the transformer to substation. This also includes overhead and underground MV conductors.
	Substation	This category includes the estimated cost of substation upgrade based on project size and interconnection voltage.
Soft costs	Overhead and profit	This includes EPC profit for all activities and overhead costs such as lodging, bonding, warranties, and insurance.
	Asset management	This category includes additional equipment, such as SCADA systems, weather stations, and underground trenching, for fiber communications cables and commissioning activities such as performance testing.
	General construction	This category includes larger construction-related expenses such as rental construction equipment, civil work, security system, and temporary ramp construction.
	Engineering	This includes engineering fees, permits, and engineering surveys.

The first step in the heuristic analysis was to collect detailed cost data from a range of utility-scale FPV projects that have been completed recently or are in the process of being deployed. This data typically includes the following:

- Total installed capacity in MW
- Total capital cost, including costs for PV modules, inverters, mounting structures, racking, anchoring and mooring, install labor, and grid connection
- Cost breakdown per component (e.g., cost per watt for PV modules)
- Geographic location as costs can vary significantly based on location, including different sales tax, labor rates, etc.
- Distance to shore to determine the type of technology used.

Next, the analysis identifies the key cost drivers for CapEx in utility-scale solar projects. These include:

- **PV module costs**: The largest component of CapEx, which has been decreasing steadily due to advancements in technology and economies of scale
- **Electrical Balance of System (EBOS) costs**: Includes inverters, racking, cabling, and other electrical components
- **Permitting costs**: Varies widely depending on location, land use regulations, and the need for environmental assessments
- **Installation and labor costs**: Influenced by local labor rates, installation complexity, and the scale of the project
- **Grid connection costs**: Dependent on the proximity to the grid and the required infrastructure upgrades.

By analyzing cost data from multiple projects, it is possible to identify trends and create a heuristic model for estimating CapEx. For instance, studies have shown that:

- **PV module prices** have dropped significantly over the past decade, with current costs averaging around $0.20 to $0.30 per watt depending on the region and technology (IRENA 2024).
- **Total CapEx** for utility-scale solar projects typically ranges between $800 and $1,500 per kW of installed capacity, depending on factors such as location, scale, and technology choices (NREL 2024).
- **Economies of scale** play a crucial role; larger projects tend to have lower per-unit costs due to more efficient uses of resources and bargaining power with suppliers.

Using the heuristic model derived from current deployments, one can estimate the CapEx for new utility-scale solar projects. For example, if a project in a region with labor rates is expected to install 100 MW of capacity, the heuristic model might suggest a CapEx range of $800,000 to $1,200,000 per MW, resulting in a total estimated CapEx of $80 million to $120 million.

The final step involves adjusting the heuristic estimates based on specific project conditions such as in the following examples:

- **Local incentives and subsidies** that could reduce overall CapEx
- **Unique geographical or environmental considerations** that might increase costs such as difficult terrain or stricter environmental regulations
- **Technological choices**, such as the decision to use tracking systems, which might increase efficiency but also raise upfront costs.

A heuristic analysis based on proprietary data from deployed utility-scale solar projects provides a practical and relatively accurate method to estimate CapEx for future projects. By continuously updating this model with new data from ongoing and completed projects, stakeholders can refine their cost estimates and make more informed decisions about the financial viability of solar investments. For example, the data in Table 5 show the ranges and the parameters considered for determining the price of the anchoring and mooring components. The price is driven by the system size, the size of the solar panels, and the module tilt. The latter influences the price because the tilt of the panels influences the wind loading in the installation, and therefore, dictates the engineering considerations for designing anchoring and mooring. This effect can be seen more clearly in Figure 13, where the cost piers and anchoring are plotted as a function of the system size. One interesting phenomenon is that for FPV systems with a capacity beyond a value of approximately 10 MW, the price does not change depending on tilt.

Table 5. Heuristics for determining the price of anchoring and mooring.

Parameter	Min	Max	Step/values
System size (kW_{AC})	1000	100,000	1,000
Module wattage (W)	545	600	545, 565, 590, 600
Module tilt (Deg)	5	15	5, 12, 15
Piers/anchoring ($/W)	0.0183	.0565	NA

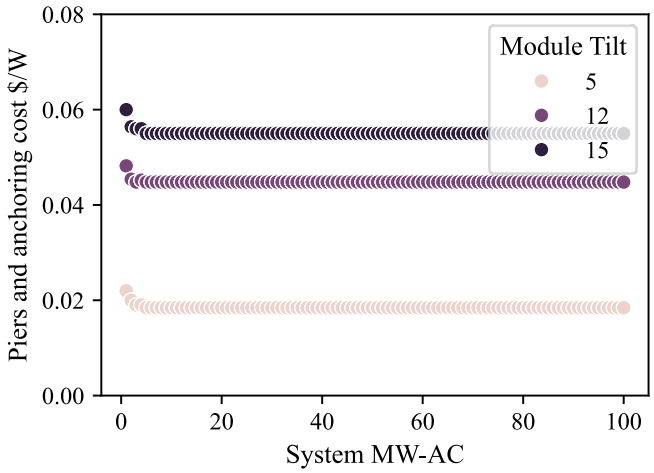

Figure 13. Graphical representation of the heuristics in the piers and anchoring category.

Another important novelty of the CapEx tool is the cost estimate of a substation upgrade of a new FPV installation. Given the organic synergies that FPV has with hydropower, the CapEx tool was designed with a hydropower operator in mind. If the proposed FPV system exceeds the capacity of the current substation, the tool has the capability to factor in the necessary upgrade costs. This ensures that stakeholders have a clear understanding of the financial requirements for such an integration, ultimately facilitating informed decision making and promoting the adoption of FPV solutions. The data in Table 6 indicate the parameters that were considered to determine the costs of upgrading a substation with specific size requirements. The driving variables are the size of the FPV system and the interconnection voltage. The two types of substations that are included are for distribution scale and for utility scale. This is determined by both the size and the interconnection voltage. Note that the range of values for the substation upgrade can significantly increase the overall CAPEX of a new FPV installation.

Table 6. Heuristics for determining the cost of a new substation.

Type	kW_AC	Interconnection Voltage (kV)	Size of Substation	Cost
Distribution Grid	0	0	NONE	$0.00
Distribution Grid	1	0	NONE	$250,000.00
Distribution Grid	20,000	34.5	NONE	$500,000.00
Utility Grid	20,000	115	4 position (1 MPT and one breaker)	$7,500,000.00
Utility Grid	100,000	161	4 position (1 MPT and one breaker)	$9,000,000.00
Utility Grid	100,000	230	6 position (2 MPT and breaker)	$20,000,000.00
Utility Grid	1,000,000	500	6 position (2 MPT and breaker)	$43,000,000.00

These examples highlight how the FPV CapEx tool can effectively provide cost estimates to stakeholders. Designed with user accessibility in mind, the tool operates at a level of complexity that does not necessitate a detailed engineering design for a specific FPV system. Instead, it offers an easy entry point for exploring cost estimates using commonly known inputs, making it a valuable resource for preliminary financial assessments in FPV projects. The tool is available to stakeholders at https://aquapv.inl.gov/CAPEX, and it has the following workflow (Figure 14): the user indicates the project size in MW_{DC}, the DC to AC factor, the panel tilt, the desired solar panel size, the solar panel cost, the inverter cost, the distance to shore, the sales tax, and whether a new substation is required. Once the inputs are defined, the tool uses an interpolation function among the multidimensional heuristics to determine the cost of each category, as shown in the outputs in Figure 14. In this case, the substation cost is zero since it was not included into the calculation.

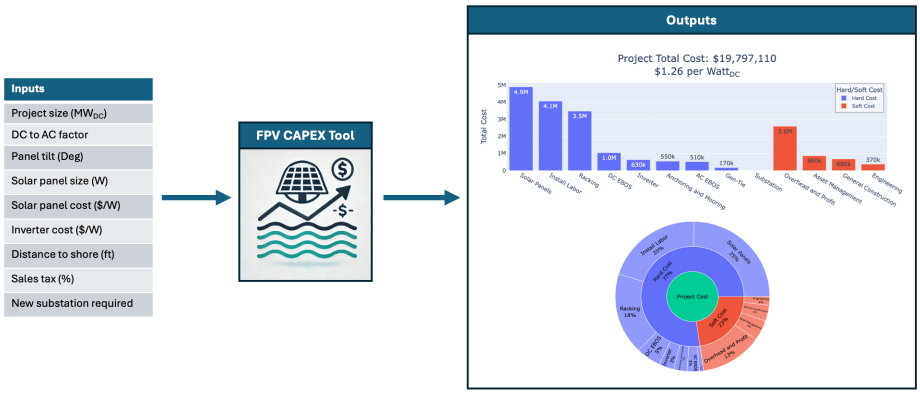

Figure 14. Workflow of the FPV CapEx tool in AquaPV.

3. CASE STUDY: THE TUCKERTOWN RESERVOIR

This section will expand on the methods to assess the TEA of FPV, through the lens of the case study of the Tuckertown Reservoir in North Carolina. This analysis could help identify the optimal conditions under which a utility-scale FPV project can thrive.

3.1. Technical Potential at Tuckertown Reservoir

These methods were applied to Tuckertown Reservoir in the United States technical potential analysis. However, in the National Hydrography Dataset Plus v2, Tuckertown Reservoir was considered as single reservoir with the neighboring High Rock Lake and Badin Lake (US EPA 2014). For the purpose of this case study, results are recalculated for Tuckertown Reservoir using the National Hydrography Dataset High Resolution (NHDHR), where Tuckertown is its own reservoir (Buto and Anderson 2020). The results of applying the national-scale methodology to only Tuckertown Reservoir using the NHDHR polygon is shown in **Error! Reference source not found.**.

Table 7. Tuckertown Reservoir national-scale methodology for FPV maximum capacity and generation.

	Developable Area (hectares)	Developable Area (percent of maximum area)	Maximum Capacity (MW_{DC})	Estimated Annual Generation (GWh_{AC})
25% Minimum Volume	224.3	24.8%	224.3	314.8
35% Minimum Volume	302.6	33.4%	302.6	424.7

As the primary inflow into the reservoir is regulated by the upstream High Rock dam and without other high flow waterway inlets, the hydrological forebay and tailrace zone exclusions are negligible. There are two dam exclusions zones because there is a dam both on the primary inlet and primary outlet. However, Tuckertown Reservoir is large enough that the 100-meter exclusion zones around High Rock and Tuckertown dams exclude less than 1% of the reservoir's area. The average slope of the reservoir floor is estimated to be over 4% above the thresholds at which it is assumed FPV floats may be designed to survive repeated grounding at low fill levels, as such the results for Tuckertown Reservoir are the same in both the 2% and 3% slope exclusion scenarios.

Because of the insignificance of the forebay, tailrace, and dam buffer exclusions and the inability to develop FPV where the reservoir may become dry due to the floor slope, the developable area estimate for Tuckertown Reservoir is almost entirely a function of the estimated surface area of the reservoir at low fill levels. However, the 25% and 35% volume cutoffs used to estimate the surface area at low fill would generally represent unusually low fill volumes for typical reservoirs in the U.S. southeast of where Tuckertown Reservoir is located. This suggests that the low fill-volume assumptions used for the national analysis may produce a poor representation of the available area for FPV development in this case study.

The operational water level of Tuckertown Reservoir as specified in its FERC license is even lower than would be suggested by its location. The agreed operational range states that the water level will be kept within 3 feet of its maximum pool (*Lake Levels – Cube Hydro Carolinas* n.d.). Although there is no long-term publicly available measurement data for the water elevation at Tuckertown, the ResOpsUS dataset contains water elevation estimates for Lake Tillery, which is downstream on the same river. These data show that the water elevation of Tilley reservoir have varied within a range of 4 feet over the last 20 years (Steyaert et al. 2022). While not direct proof of the water-level variation at Tuckertown Reservoir, the low level of water-level variation seen on the same managed riverway system gives reason to suggest that Tuckertown Reservoir is generally operated within its tight FERC license range. Therefore, the estimated area for FPV development for the reservoir is given in **Error! Reference source not found.** using this elevation for this minimum fill volume, as well as the 25% and 35% volume level cutoffs used for the national-scale technical potential analysis for comparison.

Table 8. Tuckertown Reservoir national-scale methodology for FPV maximum capacity and generation compared to FERC license operational minimum water level requirement.

	Developable Are (hectares)	Developable Area (percent of maximum area)	Maximum Capacity (MWDC)	Estimated Annual Generation (GWhAC)
25% Minimum Volume	224.3	24.8%	224.3	314.8
35% Minimum Volume	302.6	33.4%	302.6	424.7
FERC Operational Minimum	609.6	67.3%	609.3	855.2

3.2. Reservoir Considerations

The Tuckertown reservoir is located 8 miles north of Badin, North Carolina, on the Yadkin River, downstream of the High Rock reservoir (Eagle Creek n.d.). The storage capacity of the reservoir between High Rock and Tuckertown is 6,700 acre-feet at full pond elevation, and it covers a surface area of 2,560 acres. The minimum elevation that must be maintained is 561.7 feet, with a normal pool elevation of 564.7 feet. Historically, the Tuckertown plant was operated as run-of-river but has been developed to use storage capacity to increase efficiency and generation. The Tuckertown powerhouse has three 12.68 MW vertical Kaplan units totaling 38.04 MW. The station interconnects to a substation onsite rated for 21 (3 × 16) MVA, 6.9/115 KV transformers. Tuckertown is monitored for instantaneous dissolved oxygen (DO) levels, daily average DO levels, and water temperature. Currently, there is a 200-ft setback from the dam, and substation (Figure 15), which should be respected during the FPV design process.

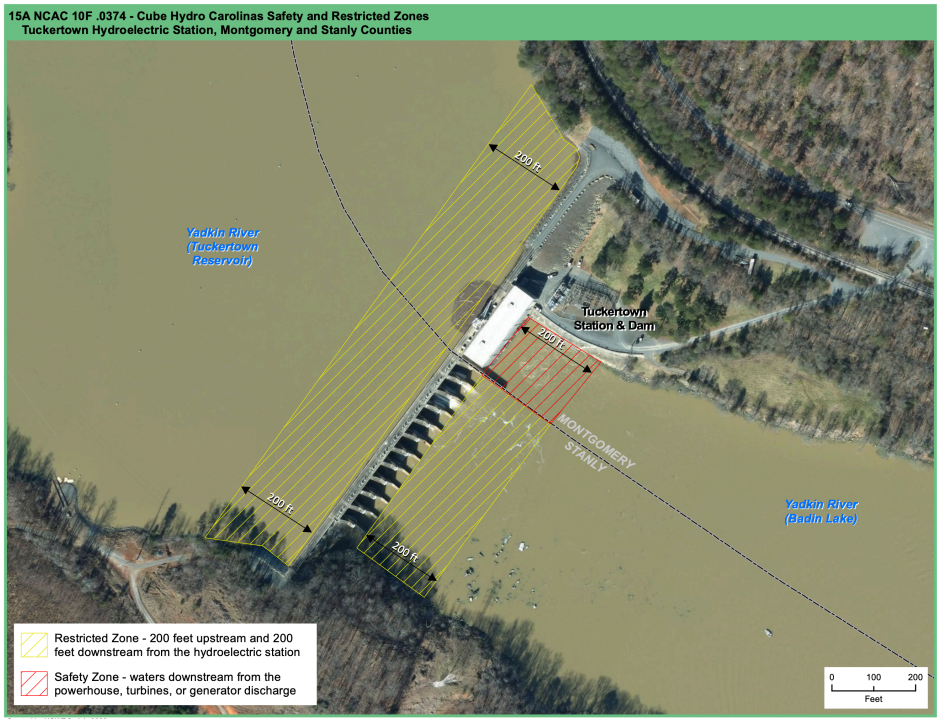

Figure 15. Restrictive zones along the Tuckertown station and dam.

3.2.1. System considerations prior to FPV design

The design of an FPV system for the Tuckertown reservoir was made considering the existing infrastructure of the power system along the Yadkin River Hydroelectric Project, and across three hydropower plants: Badin, Tuckertown, and High Rock with the purpose of developing a hybrid FPV-Hydro power plant. The two main system considerations that can limit the size of the FPV system are the transmission capacity and the substation capacity. This is independent of whether the plant would be a co-located independent system or a co-located integrated hybrid (Figure 16). Out of these two considerations, the transmission capacity should be the starting point since it has physical limitations as to how much additional capacity the current infrastructure would sustain. The substation capacity also has physical limitations, but those can be overcome more easily if the investment of a substation upgrade is deemed feasible (see Section 2.3 for more details on technoeconomic). In this section, the focus is to determine what is the maximum capacity of an FPV plant at the Tuckertown reservoir that does not compromise the reliability of the system along the Yadkin River Hydroelectric Project.

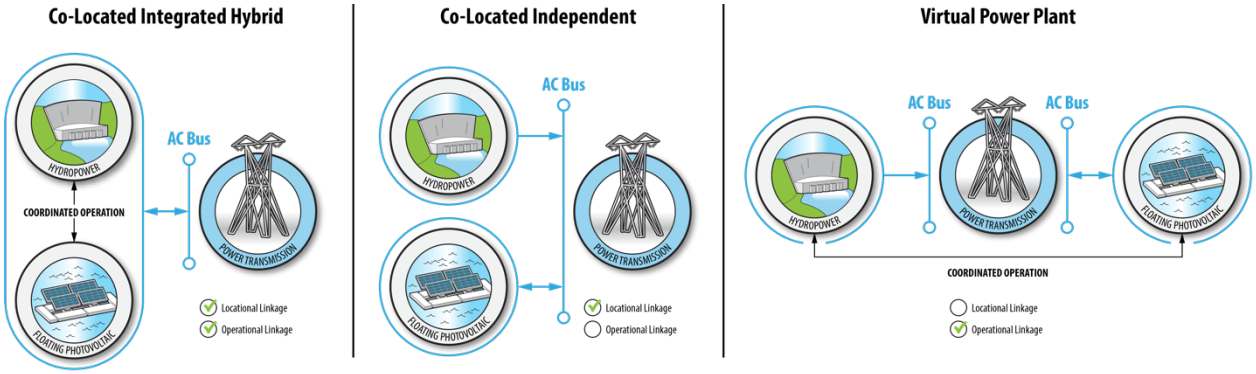

Figure 16. Three topologies of multi-energy systems.

Eagle Creek Renewable Energy (ECRE) conducted a steady-state analysis of five scenarios for the co-location of FPV with hydropower at Tuckertown, where the capacity ratios of FPV to hydro were varied to understand the limits in the existing infrastructure, namely the 100 kV transmission lines between Badin, High-Rock, and Tuckertown. An example of the business-as-usual (BAU) case is given in (Figure 17), where the three transmission lines connecting each power plant are included, along with their carrying capacity. The parameters, *Pgen* and *Pmax,* denote the generation of a given plant in the scenario and the maximum plant capacity, respectively. Note that the FPV plant has been added to the Tuckertown substation as "Tuckertown PV." The color-coded circles between the transmission indicate the percentage capacity used for the scenario (e.g., a 50% indicates that only half of the capacity of the 100-kV line is being used). The colors indicate whether the load is acceptable and within safe operating conditions: green is acceptable, yellow indicates the capacity is approaching a load threshold of 90%, and red indicates a loading above 90%, which is unacceptable. Additionally, four buses are attached to the Badin junction, which carry generated capacity from other power plants outside of ECRE's jurisdiction. The direction of the arrows indicates whether the generation from these plants is going into the transmission line from Badin to High Rock (left to right arrow) or the opposite direction. The numbers along the transmission lines are the total capacity in the scenario. For example, the BAU case in Figure 17 shows 4.18 MW generation at the Narrows plant, while the rest is zero. Yet, the transmission lines are carrying over 50% of their capacity. This is because approximately 60 MW of generation are coming from adjacent power plants through the buses at Badin. Therefore, the steady-state analysis considers the optimal balancing in the grid, including typical generation of ECRE's power plants and others.

Based on the description above, the considerations for each scenario are as follow:

1. **Scenario 1:** This BAU case intends to show the loading in the transmission lines by considering a typical operation condition of the system. Note that the value of Pmax of Tuckertown PV (i.e., the FPV) is zero for this scenario. The green color in the circles indicate that in this case, the system is operating with an acceptable loading and includes capacity from other power plants (Figure 17).
2. **Scenario 2:** All the hydropower plants are operating at the maximum capacity and approximately 97 MW are distributed from Badin to other transmission lines via the buses. This is conducive to a loading on the Tuckertown-High Rock transmission line of 79%, and it is within the acceptable loading. In this case, the FPV system capacity is zero (Figure 18).
3. **Scenario 3:** All the hydropower plants are operating at full capacity in addition to the FPV plant in Tuckertown, with a capacity of 33 MW. This is the scenario that enables the use of the existing 6.9 kV substation and a safe operation of the system. Even with a loading approaching the threshold at 88%, it is within the safety margin for a balanced grid. Additional generation is sent from Badin to other transmission lines. This is the optimal scenario for adding an FPV plant to Tuckertown (Figure 19).
4. **Scenario 4:** This is a very similar configuration as in Scenario 3,[c] but with a FPV capacity of 51 MW. This yields a high loading in the transmission line between Tuckertown and High Rock by reaching 93% of the capacity, which is deemed as high loading.
5. **Scenario 5:** This is an extreme case where the braker from Tuckertown to High Rock is opened, and therefore, generated power from Tuckertown will be send back to Badin. The FPV capacity in this scenario is 45 MW. It is worth noting that this strategy is only applied in extreme scenarios, and it is **not accepted as a normal operating procedure** (Figure 20**)**.

c A figure for this scenario is not included for the sake of brevity.

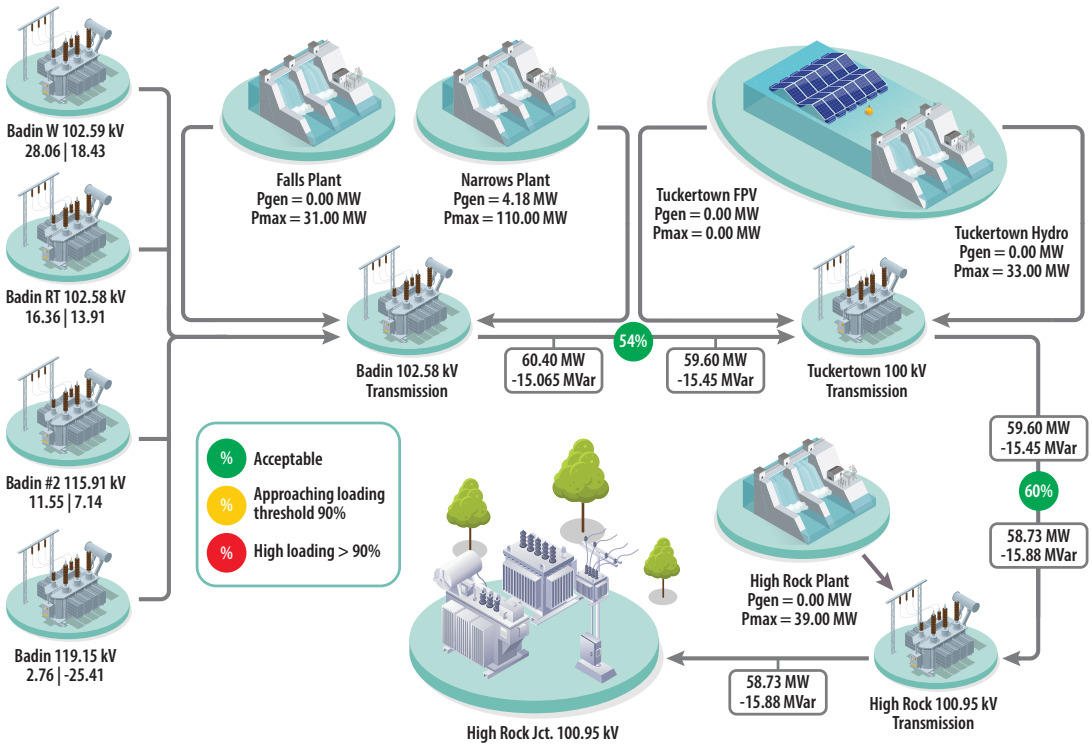

Figure 17. Scenario 1: Layout of hydropower plants along the Yadkin River and operated by ECRE. The three plants are connected with 100 kV transmission lines. The values of capacity and generation in this example are BAU case.

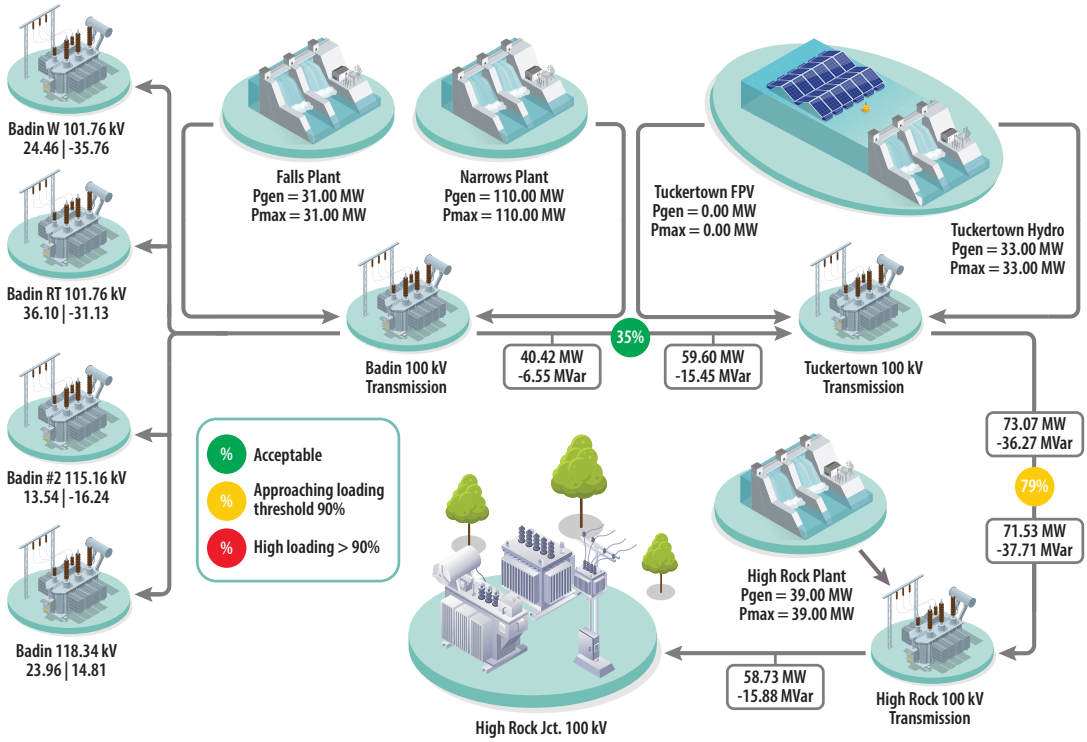

Figure 18. Scenario 2: Capacity share.

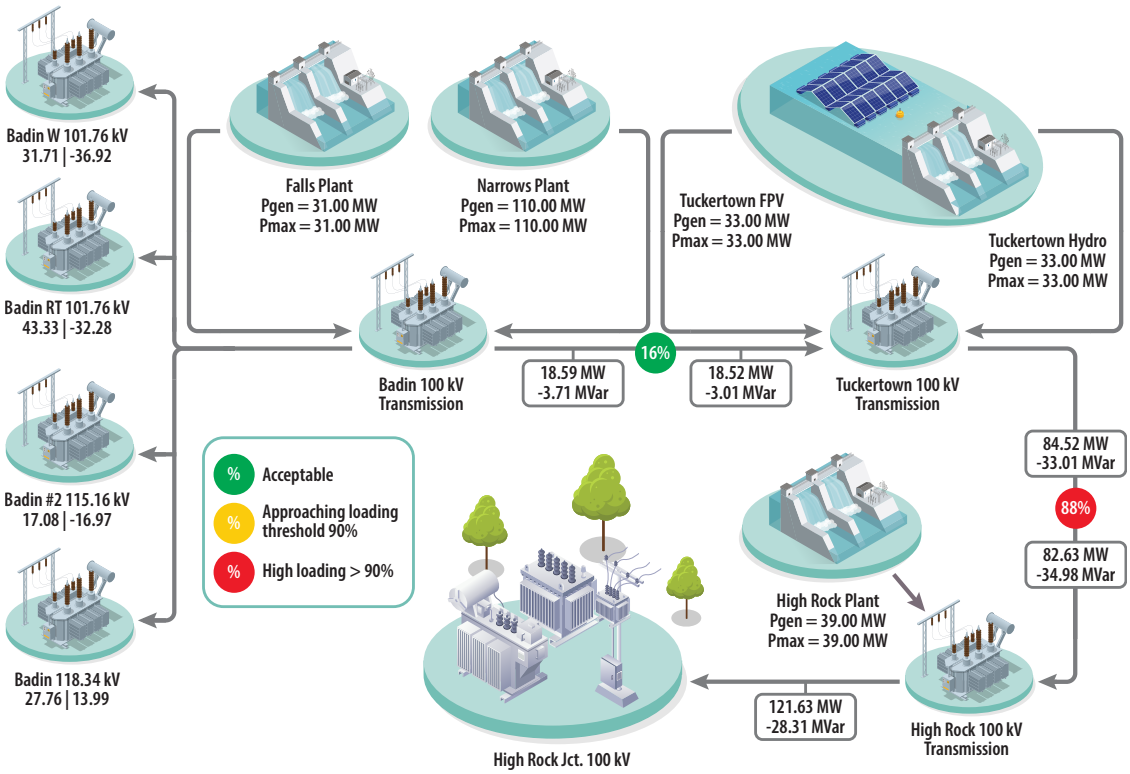

Figure 19. Scenario 3: The steady-state analysis of the chosen FPV capacity.

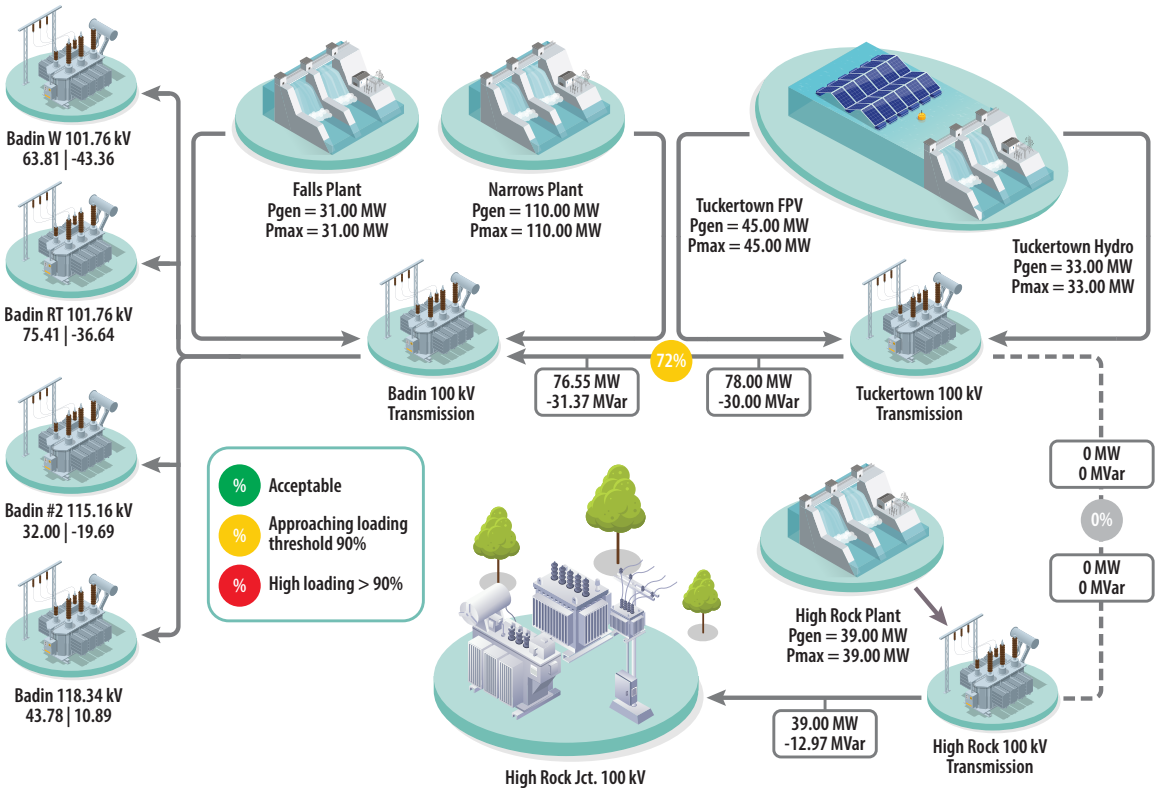

Figure 20. Scenario 5: When a circuit braker is open between Tuckertown and High Rock to prevent instabilities in the grid due to the high capacity generated in this configuration.

As indicated above, the most favorable configuration given the existing infrastructure is when the FPV system has a maximum generating capacity of 33 MW_{AC}. Based on this, Det Norsk Veritas (DNV) proceeded to design the optimal layout of the FPV panels in the Tuckertown reservoir, considering the setbacks to the shore and dam, as well as a 100 ft. easement from transmission lines. Additional considerations included a debris diversion system, which would direct any debris transported by the river into a cove west of the FPV array with a 50 ft. setback.

3.2.2. CO-LOCATED DESIGN: 33 MW

The layout of the FPV system (Figure 21) contains 9 × 3.667 MW inverters installed in an equipment pad onshore with an integrated 690 V/6.9 kV step-up transformer. The inverters are connected through a three-circuit 6.9 kV overhead collector system. The existing substation in the Tuckertown down is used for the interconnection at the 6.9 kV point of interconnection, where each 6.9 kV circuit connects to the substation through the addition of three circuit breakers, applicable protection relays, and metering equipment. An example of the FPV racking is shown in Figure 22. Each module is installed in landscape mode, with 12^0 tilt, 0.72 GCR (ground coverage ratio), and due south azimuth.

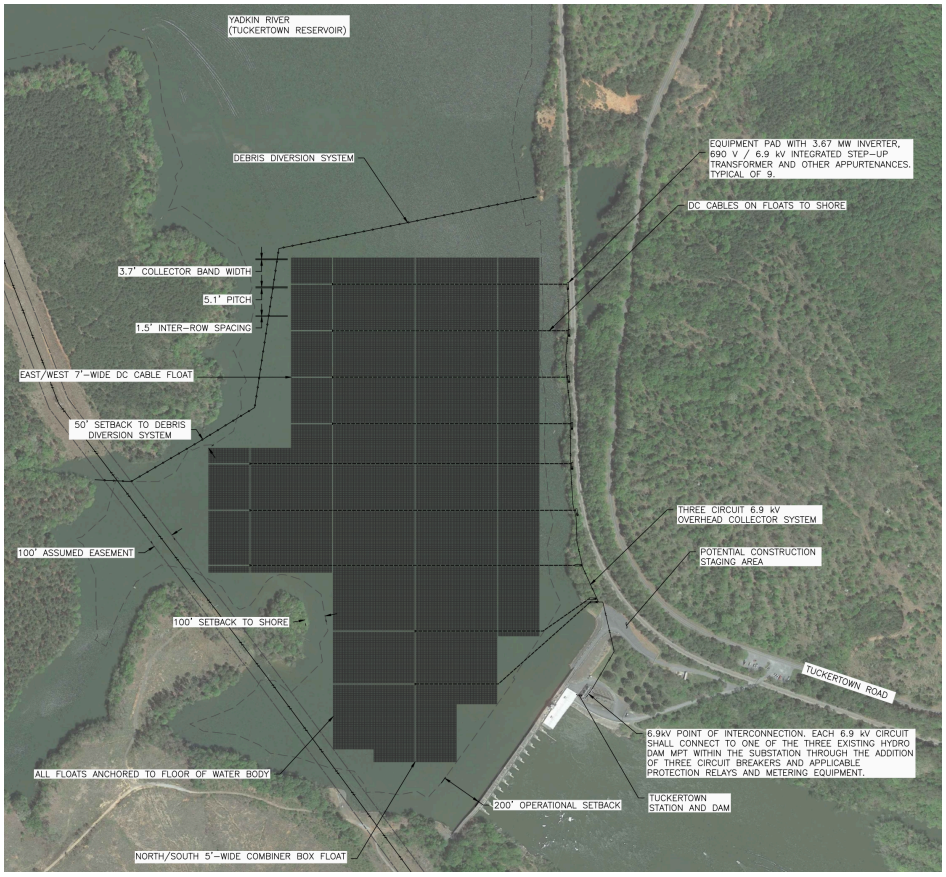

Figure 21. The 33 MW FPV system designed by DNV.

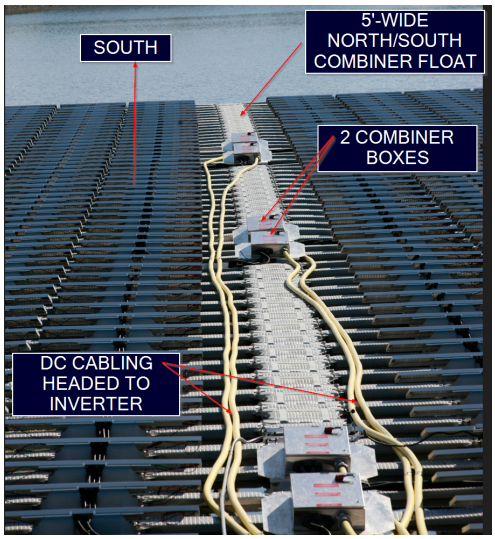

Figure 22. An example of the configuration and racking in an FPV island.

3.3. Techno-economic Assessment

Specifically, regarding the Tuckertown reservoir, this section will explore the techno-economic assessment of the 33 MW_{AC} design described in Section 3.2.1. In general, a complete TEA for FPV using the AquaPV toolkit will follow the workflow described previously in Figure 12. For the 33 MW_{AC} design in the Tuckertown reservoir, the hourly solar generation is determined using the AquaPV Solar Generation tool (INL n.d.) which is a wrapper to the open-source tool pvlib. The results shown in Figure 23 and Figure 24 show the hourly and monthly generation, respectively. Note that the hourly generation is capped at 33 MW_{AC} due to the DC to AC ratio of 1.3 and the system size specification of 41.2 MW_{DC} (Table 9).

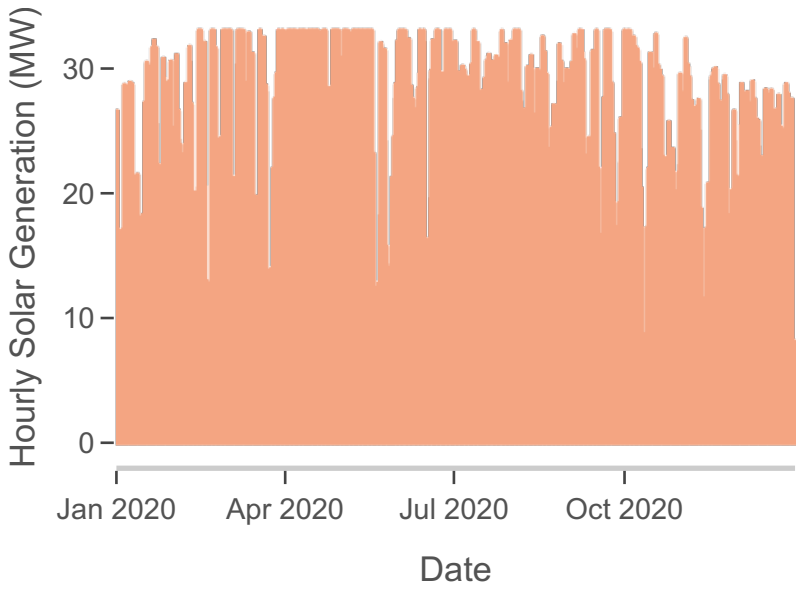

Figure 23. The hourly generation for a typical year at the Tuckertown reservoir. This corresponds to a 41.2 MW_{DC} capacity. Note that the generation is clipped at 33 MW_{AC}.

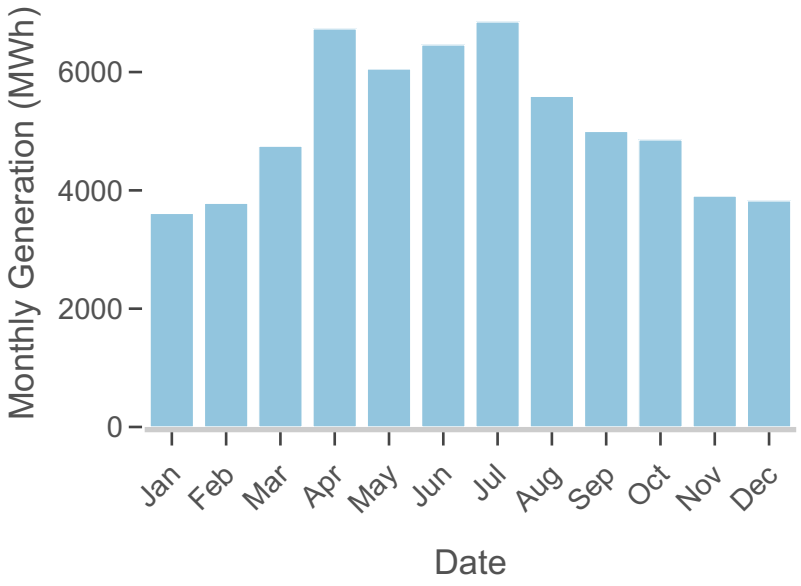

Figure 24. The monthly generation for a typical year at the Tuckertown reservoir.

Table 9. The input values specific to the Tuckertown reservoir FPV design.

Parameter	Value
Capacity [MW_{DC}]	41.2
DC to AC ratio [-]	1.3
System efficiency [%]	98
Tilt [Deg]	12
Module wattage [W]	600
Module price [$/W]	0.31
Inverter price [$/W]	0.04
Distance to shore [ft]	100
Substation upgrade [-]	Yes
Connection voltage [kV]	16

Next, the baseline CapEx (Table 10) of the system is determined based on the inputs in Table 9, which follow the design presented in Section 3.2.2. Since the size of the system is large enough to require its own substation, the CapEx value reflects that in the Substation category with a total value of $500K. The largest hard cost incurred are the panels, with a total of $13.6M, while the largest soft cost is under the Overhead and Profit category, with a total of $5.6M. The total cost of the project is $52.6M, with a cost of $1.19 per watt.

Table 10. Breakdown of the CapEx for Tuckertown.

CapEx	Cost [$/W_DC]	Total Cost [$]
Solar Panels	0.265	13,666,040
Install Labor	0.255	10,514,240
Racking	0.226	9,294,740
Overhead and Profit	0.137	5,656,137
DC EBOS	0.068	2,785,125
Asset Management	0.055	2,253,690
Inverter	0.034	1,763,360
Engineering	0.040	1,646,682
Anchoring and Mooring	0.035	1,450,240
AC EBOS	0.032	1,337,332
General Construction	0.030	1,252,480
Substation	0.010	500,000
Gen-Tie	0.011	453,513
Project Cost	1.199	52,573,578

Revenue is determined by considering the price of electricity at a nearby locational marginal pricing (LMP) serviced by PJM. To approximate future electricity market information in the next 20–30 years, probabilistic electricity price forecasting is adopted, which measures the market uncertainty, and therefore, directly impact the techno-economic assessment (Sun 2024). In this report, only long-term temperature forecasts data from Burleyson et al. (Burleyson 2023) are used since temperature is by nature the driver of electricity demand and price (Jasiński n.d.). Details about temperature data and demand data are described in (Sun 2024). Once the electricity price drivers are determined, the long-term electricity price forecasts can be generated by the trained SVR mode. To this end, 100 hourly LMP price scenarios were generated from 2022 to 2040. The time series in Figure 25 shows the predicted LMP price for one day, Figure 26 depicts the average predicted price over the entire period, and Figure 27 provides the predicted prices for all the scenarios on a seasonal basis.

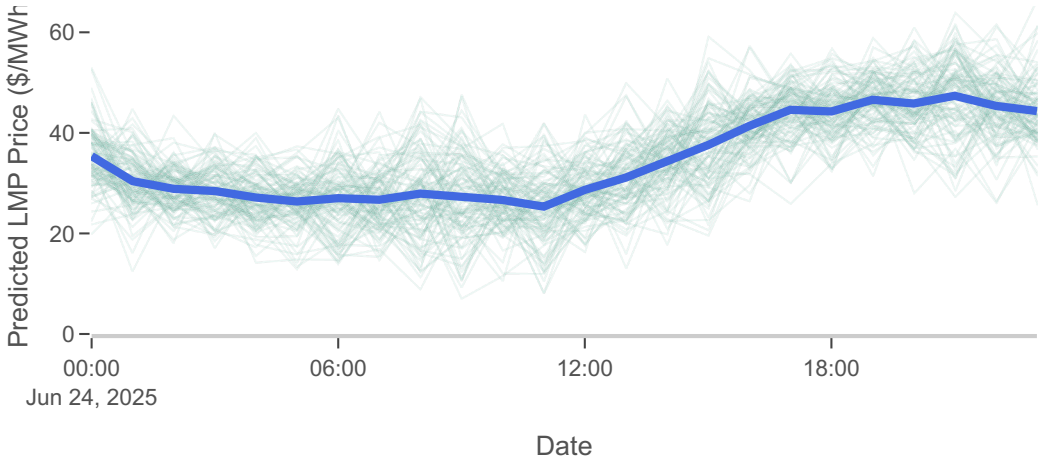

Figure 25. Example price for one day in the summer. The blue line is the average price, while the gray lines are the scenarios.

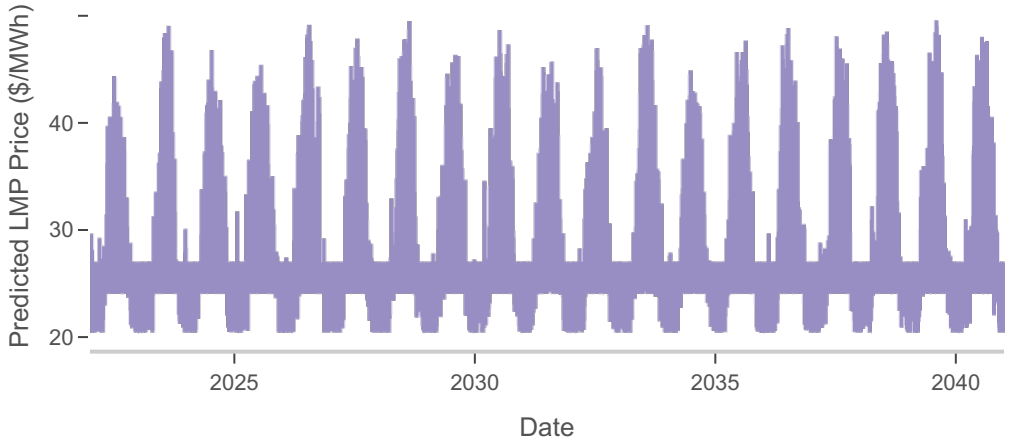

Figure 26. Predicted LMP price for the next 30 years.

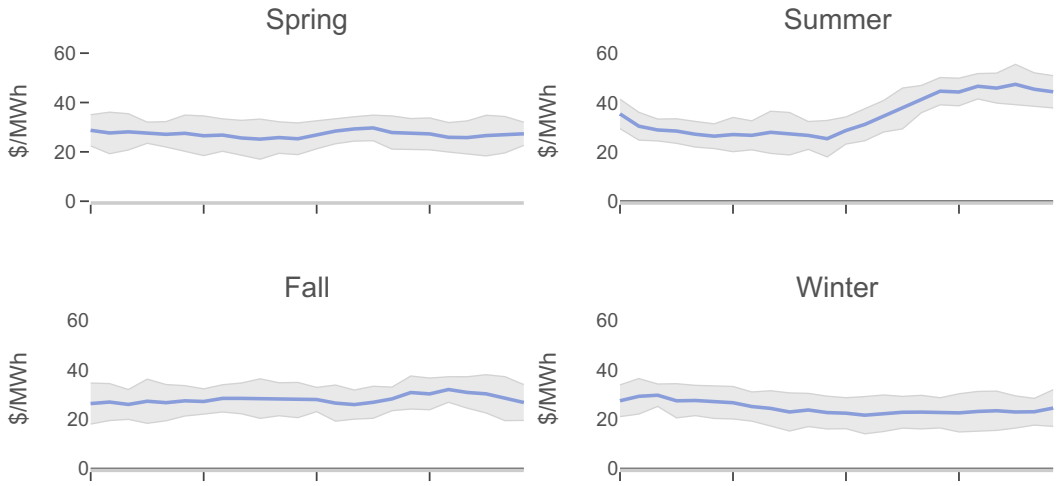

Figure 27. Seasonal price change for all scenarios in the LMP.

As described in Figure 12, the revenue is determined using the hourly generation and the predicted energy price for the next 30 years for 100 scenarios. Next, the financial metrics are computed to determine the financial viability of the project. AquaPV provides the LCOE, payback period, NPV, and ROI. For each of the 100 electricity price scenarios, it is possible to generate a range of results with associated uncertainty considering the following variables:

- Include the investment tax credit (ITC) as 30%[d]
- Include the production tax credit (PTC) for 10 years as 2 cent/kWh[d]
- No incentives are applied
- Life expectancy of 30 years
- An annual discount rate of 7%
- High and low estimates of CapEx and OpEx by adding/subtracting 5%.

The ranges for each financial metric are presented in Table 11. As expected, the federal incentives have a positive impact on the feasibility of the project by bringing the LCOE down from $50.20/MW to $31.08/MW. The NPV for all scenarios is below zero, except for when pricing scenarios higher than the mean and when incentives are applied. Similarly, if no federal incentives are applied, the payback period gets close to the life of the system. In the best case scenario, the project is expected to pay for itself in nearly 16.55 years before returning a profit. Among the federal incentives, the ITC is the most favorable given that this project requires a high capital investment up front. The cells highlighted in green in Table 11 indicate favorable results due to the higher electricity price.

Table 11. TEA results for the 41.2 MW design at Tuckertown.

	Minimum			Maximum		
Financial Metric	ITC	PTC	None	ITC	PTC	None
LCOE ($/MW)	31.08	32.52	45.42	35.86	37.30	50.20

[d] Although H.R. 1 (enacted July 2025) shortened the eligibility window for IRA's clean-energy credits—requiring wind and solar projects to begin construction within 12 months of enactment and be completed within four years or, if a project missed the construction start window, be placed in service by 2027—Investment Tax Credit (ITC) and Product Tax Credit (PTC) provisions remain in effect for qualifying technologies for several more years under current Treasury guidance. The deadline for project completion is further extended to ten years for projects on federal lands.

Payback period (years)	16.55	16.13	24.29	22.40	21.68	29.86
NPV ($M)	-7,68	-9,27	-23,4	2,90	0.13	-12,86
30-year ROI (%)	55.44	57.54	23.88.1	24.53	26.43	-4.02
IRR (%)	4.74	4.28	1.54	2.17	2.09	-0.28

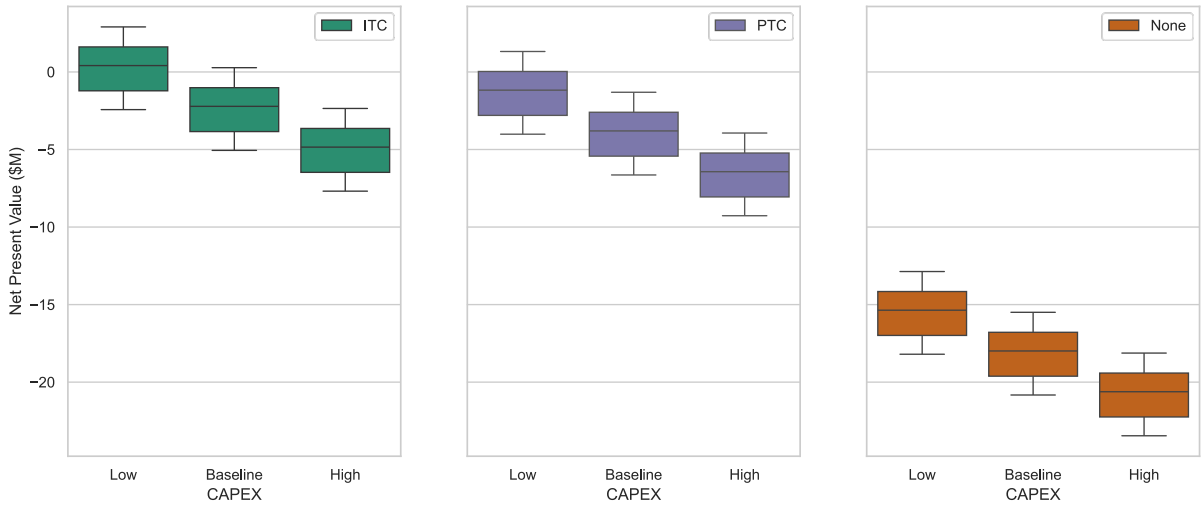

Figure 28. The NPV for the case study. On the scenario with a -5% from Baseline of CapEx, the project has the chance to be feasible.

3.3.1. Regulatory Considerations for Tuckertown

The Tuckertown Reservior includes one of four hydropower developments within the Yadkin Hydroelectric Project license (P-2197) (hereafter Yadkin Project) on the Yadkin River. The Yadkin project was originally licensed in May of 1958 by the Federal Power Commission and received a 50-year license by the Federal Energy Regulatory Commission (FERC). After the original license expired in 2008, the Yadkin Project received several annual licenses due to prolonged settlement agreement negotiations before issuing a new license for the Yadkin Project in September 2016. The new 38-year license from FERC for the Yadkin Project does not expire until March 31, 2055.

Generally, FERC has regulatory authority over the construction, operation, and maintenance of FPV developed within the jurisdictional boundary (FERC license boundary or project boundary) of a FERC-licensed non-federal hydroelectric project (Levine 2024). Proposed and existing non-federal hydroelectric projects subject to FERC jurisdiction can add FPV through three regulatory pathways: (1) an original license that proposes to construct a co-located hydroelectric and FPV project, (2) a new license (relicense) of an existing hydroelectric project that proposes to co-locate FPV with the existing hydroelectric project, or (3) a non-capacity amendment to an existing license to co-locate FPV with the hydroelectric project utilizing project lands and waters (Levine 2024). In the case of the Tuckertown Reservoir within the Yadkin license, the most likely of these regulatory pathways would be a non-capacity amendment since the current FERC license does not expire until March 31, 2055.

The type of non-capacity amendment required for the addition of co-located FPV with an existing FERC-licensed hydroelectric project depends on whether the FPV will be operationally paired with the hydroelectric project (Levine 2024). A developer needs a non-capacity amendment to construct, operate, and maintain an FPV project that is co-located and determined to be “a miscellaneous structure used and useful” (i.e., operationally paired) in connection with an existing FERC-licensed hydroelectric project

(16 U.S.C. §§ 791–823g; 18 C.F.R. §§ 4.200–4.202; FERC 2015; Levine 2024). However, if the FPV is not determined to be a miscellaneous structure used and useful(i.e., operationally paired) in connection with an existing FERC-licensed hydroelectric project, a developer needs a non-capacity amendment for Non-Project Use. This type of non-capacity amendment is required to construct, operate, and maintain an FPV project that is co-located on lands and waters within the FERC license boundary, but is not considered a miscellaneous structure sed and useful" (i.e., not operationally paired) in connection with an existing FERC-licensed hydroelectric or PSH facility (16 U.S.C. §§ 791–823g; 18 C.F.R. §§ 4.200–4.202; FERC 2015; Levine 2024).

In addition to the required FERC authorizations under the Federal Power Act, a number of other authorizations/processes are required under federal law when FERC issues an original or new license, and may be required for a non-capacity amendment if warranted under the specific circumstances. These authorizations/processes include compliance with the Clean Water Act, Endangered Species Act, National Historic Preservation Act, and National Environmental Policy Act (see Levine 2024 for more detail https://www.nrel.gov/docs/fy24osti/86325.pdf).

3.3.2. Environmental Considerations

Once general environmental interactions have been identified in a stressor-receptor table, as described above, a site/project-specific investigation is needed to determine what local habitats/biota are present and are likely to be susceptible to the effects of project components and subsequent environmental changes. In this case study for a potential FPV project associated with Tuckertown Dam,species were identified, which are likely to be present in the Tuckertown Reservoir that may have specific ecological, management, and/or recreational concern within each of the receptor categories (Table 12) based on Draft License Agreement and Environmental Impact Statement documents for the Yadkin (FERC No. 2197) and Yadkin-Pee Dee River (FERC No. 2206) Hydroelectric Projects available on the FERC docket and from literature reviews and web searches. In an actual permitting process, subject matter experts would be consulted to determine species of likely interaction. In a stressor-receptor approach, the interaction cells are often ranked or colored by the level of concern based on expert opinion of the likelihood, frequency, and scale of consequence of the interaction as well as regulatory stringency and, potentially, stakeholder concern (e.g., Klure et al. 2012, Exley et al. 2021).

Table 12. Taxa within each of the receptor categories potentially present in Tuckertown Reservoir.

Receptor Category	Taxa reported from Tuckertown
Native SAV	Spatterdock, white water lilies, American pondweed, American lotus, coontail, Water willow *Justicia americana*
Noxious SAV	Hydrilla
Algae/Blue-green algae	Lyngba, Spirogyra
Sediment-inhabiting flagellates	Trachelomonads, green euglenoids, Chamydomonads, chrysophytes and cryptomonads
FW mussels	Paper pond shell (*Utterbackia imbecillis*)
Invasive invertebrates:	Mystery snails: (*Bellamya [Cipangopaludina] japonica*) is widespread in Tuckertown; one B. *chinensis* was observed on the shoreline of High Rock reservoir, 231 were counted in the Highrock tailwaters. Asian clams (*Corbicula fluminea*) are abundant in Tuckertown. Zebra mussels are not reported from the reservoir.
Other invertebrates	At the Yadkin Project, 6 phyla, 24 orders, and 41 families represented by 99 benthic macroinvertebrate species were found in the four project tailwaters.

Receptor Category	Taxa reported from Tuckertown
	Dominant taxa (other than Asian clams) include: *Dugesia tigrine*, *Musculium transversum*, *Caecidotea* sp. *Dicrotendipes simpsoni*, *Glyptotendipes*, sp.
Fish of recreational interest	Largemouth bass, Striped bass, White bass, Flathead catfish, Channel catfish, Blue catfish, Bluegill, White perch, White crappie, Black crappie
Other fish	Longnose gar, Bowfin, Gizzard shad, Threadfin shad, Blueback herring, Alewife, Common carp, Goldfish, Golden shiner, Bluehead chub, Eastern silvery minnow, Satinfin shiner, Spottail shiner, Spotted sucker, White sucker, Quillback, Creek chubsucker, Smallmouth buffalo, Silver redhorse, Shorthead redhorse, Yellow bullhead, Flat bullhead, Snail bullhead, White catfish, Black bullhead, Brown bullhead, Eastern mosquitofish, Redbreast sunfish, Warmouth, Green sunfish, Bluegill, Pumpkinseed, Redear sunfish, Smallmouth bass, Yellow perch, Tesselated darter, Johnny darter
Fish of conservation concern	Shortnose sturgeon is a migratory marine fish that once spawned in the river but has not been spotted in the basin since 1985. Currently only occur downstream of Blewett Fall dam.
Turtles	Mississippi map turtle (*Graptemys pseudogeographica kohni*), Yellow-bellied (pond) slider (*Trachemys scripta*), Painted turtle, (*Chrysemys picta*), possibly Spotted turtle (*Clemmys guttata*)
Fouling biota	
Insects	Mayflies (Ephemeroptera), stoneflies (Trichoptera), dolichopodid dipterans, and tabanid flies (Tabanidae)
Birds	Bald eagles, Great blue heron, White pelicans, Osprey, Kingfisher, Cormorant, Scoters, Eiders, Long-tailed ducks, Wood ducks, Mallards, Redheads, Canvasbacks, Black ducks, Pintail, Mottled duck, Fulvous whistling duck, Harlequin ducks, Coots, Tundra swans, Canada geese

One can compare the ecological preferences/tolerances of these species (if available) to the scale of expected changes in environmental conditions of various scenarios, as modeled by CE-QUAL-W2, for a proxy reservoir. For this Open-Loop Reservoir System, the J. Percy Priest Reservoir located in Tennessee was selected as the proxy for Tuckertown due to it being in a similar geographic region and mapping near to each other in PCA space (Figure 9 and Figure 10). As described previously, a suite of response variables was modeled in response to varying levels of surface coverage. Response variables for model iterations of 5–40% coverage (as this is a more realistic range of coverage) were extracted for winter (Jan–Feb) and summer (Jul–Aug) seasons and scaled to the percent change from the reference baseline model (Table 13). Graphs of the response variables for all model iterations (5–100%) are provided (Figure 29 through Figure 37) to visualize overall trends.

According to the Yadkin DLA, low temperatures of ~ 8°C are found in winter with summer highs of about 30°C. Weak thermal stratification of up to 4°C occurs in the summer, generally from July to September, when cooler bottom waters also had lower DO concentrations and were generally more turbid with greater concentrations of suspended solids, total phosphorus, and ammonia. Actual water temperature and DO measurements are available for Tuckertown reservoir for the summer months of 2006, 2007, 2011, 2012, 2016, 2019, and 2021. January to Feburaty data are not available for Tuckertown. However, measurements are available from High Rock reservoir (upstream from Tuckertown) monthly from 2000 to 2019. Summer water temperatures were similar on average between the two reservoirs (26.6°C for Tuckertown vs. 27.5°C for High Rock; Table 14); although, they were statistically significantly different due to the wider range of temperatures measured in Tuckertown over

the summer ($p = 0.025$, two-tail paired two sample t-test). Since summer averages were similar, winter conditions at High Rock were used as a proxy for Tuckertown.

Overall, predicted temperature changes due to coverage by FPV are not likely to represent an impact to fish habitat suitability in this reservoir. Summer temperatures are predicted to decrease. However, given the overall warm conditions of the lake, the model did not predict any decrease in warmwater fish habitat in the summer; in fact, warmwater fish habitat was predicted to increase in summer. As temperatures also were predicted to decrease in winter, there was a small, predicted decline in warmwater fish habitat in the winter, but the percent reduction was less than 1%. Coldwater fish habitat was not predicted to change, indicating that the declines in minimum temperatures predicted in summer and winter were not below thresholds for cold-adapted species. DO maxima were slightly affected but were on the order of less than 1 mg/L, with slightly greater but still miniscule declines in winter; dissolved oxygen minima were not affected in summer or winter. The biggest changes were observed in higher average DO in the summer, which is likely to be a positive outcome for most aquatic species.

Even if the available habitat for species does not change, one might consider potential changes to the performance of organisms. The spawning temperatures are provided for 14 of the 46 fish species listed in the Yadkin DLA. Two of these species, threadfin shad and golden shiner, spawn through August, the period for which this report has modeled reservoir changes due to coverage by FPV. The threadfin shad has a spawning temperature of 21°C while the Golden shiner spawns in 20–26.67°C. As summer temperatures (on average) already exceed the preferred spawning temperature for these species, a decline of 1.84–6.04°C in maximum temperature (Table 13) as a result of shading by FPV panels may be considered beneficial to reproduction for these species. Similar investigations of the match or mis-match between environmental conditions realized after coverage by FPV and the environmental tolerances or preferences of species of interest or concern could be conducted to determine expected direction and magnitude of change. This type of consideration could be applied to various species of interest when a triggering or threshold environmental condition is known.

> *This is not intended to be an Environmental Impact Assessment of a proposed FPV project on this reservoir but rather an example of how one might use the stressor-receptor framework and outputs from the CE-QUAL-W2 modeling efforts.*

Table 13. The change in response variables in J Percy Priest Reservoir, Tennessee, for FPV coverage ranging from 5–40%. The response variables are separated by seasons of summer (months July and August) and winter (months January and February).

Response Variable	Season	5%	10%	15%	20%	25%	30%	35%	40%
coldwater.fish	summer	0.00	0.00	0.00	0.00	0.00	0.00	0.00	0.00
	winter	0.00	0.00	0.00	0.00	0.00	0.00	0.00	0.00
do.max*	summer	0.19	-0.03	0.02	0.05	-0.03	-0.01	-0.06	-0.06
	winter	-0.05	-0.08	-0.06	-0.09	-0.09	-0.12	-0.10	-0.15
do.mean	summer	0.18	0.17	0.19	0.19	0.18	0.17	0.15	0.17
	winter	0.00	0.00	0.00	0.00	0.00	-0.01	0.00	-0.01
do.min*	summer	0.00	0.00	0.00	0.00	0.00	0.00	0.00	0.00
	winter	0.05	0.01	0.00	0.02	0.00	0.01	0.02	0.00
mean.outflow.temp	summer	-0.01	-0.02	-0.04	-0.04	-0.05	-0.08	-0.08	-0.09
	winter	-0.03	-0.06	-0.10	-0.11	-0.11	-0.14	-0.14	-0.16
mean.surface.temp	summer	-0.01	-0.01	-0.03	-0.03	-0.03	-0.05	-0.05	-0.06
	winter	0.00	0.00	-0.01	-0.01	-0.02	-0.03	-0.03	-0.04
range.outflow.temp*	summer	-0.08	-0.09	-0.15	-0.15	-0.16	-0.25	-0.24	-0.24
	winter	-0.05	-0.06	-0.07	-0.08	-0.07	-0.09	-0.10	-0.10
schmidt.stability	summer	-0.11	-0.16	-0.26	-0.28	-0.30	-0.35	-0.36	-0.40
	winter	-0.42	-0.55	-0.50	-0.54	-0.53	-0.59	-0.58	-0.50
stratified.days	summer	0.00	0.00	0.00	0.00	0.00	0.00	0.00	0.00
	winter	-0.05	-0.07	-0.08	-0.12	-0.12	-0.12	-0.12	-0.10
temp.max*	summer	-1.84	-2.55	-3.92	-4.16	-4.38	-5.34	-5.41	-6.01
	winter	-0.45	-0.65	-0.92	-0.98	-1.01	-1.23	-1.27	-1.34
temp.mean	summer	-0.01	-0.02	-0.05	-0.06	-0.06	-0.09	-0.09	-0.10
	winter	-0.03	-0.05	-0.09	-0.10	-0.10	-0.13	-0.13	-0.14
temp.min*	summer	-0.06	-0.12	-0.28	-0.30	-0.33	-0.62	-0.60	-0.74
	winter	-0.20	-0.36	-0.63	-0.68	-0.71	-0.88	-0.91	-1.02
thermocline.depth	summer	0.26	0.32	0.26	0.24	0.20	0.23	0.22	0.16
	winter	-0.03	0.03	-0.25	-0.62	-0.57	-0.79	-0.80	-0.86
warmwater.fish	summer	5.95	7.29	9.18	9.24	9.18	10.04	9.96	10.03
	winter	-0.08	0.02	-0.07	-0.12	-0.13	-0.16	-0.17	-0.22

* The change is expressed generally as percent change; absolute change noted by an asterisk.

Table 14. Maximum, average, and minimum water temperatures and DO concentrations in Tuckertown and High Rock reservoirs during summer (May–September) and winter (November–February) 2006–2022.

	Tuckertown summer	High Rock summer	High Rock winter
Temperature (°C)			
Max	31.80	31.30	21.00
Avg	26.64	27.48	9.69
Min	19.55	21.41	2.00
Dissolved Oxygen (mg/L)			
Max	12.60	11.15	
Avg	7.15	9.67	
Min	1.92	7.1	3.4

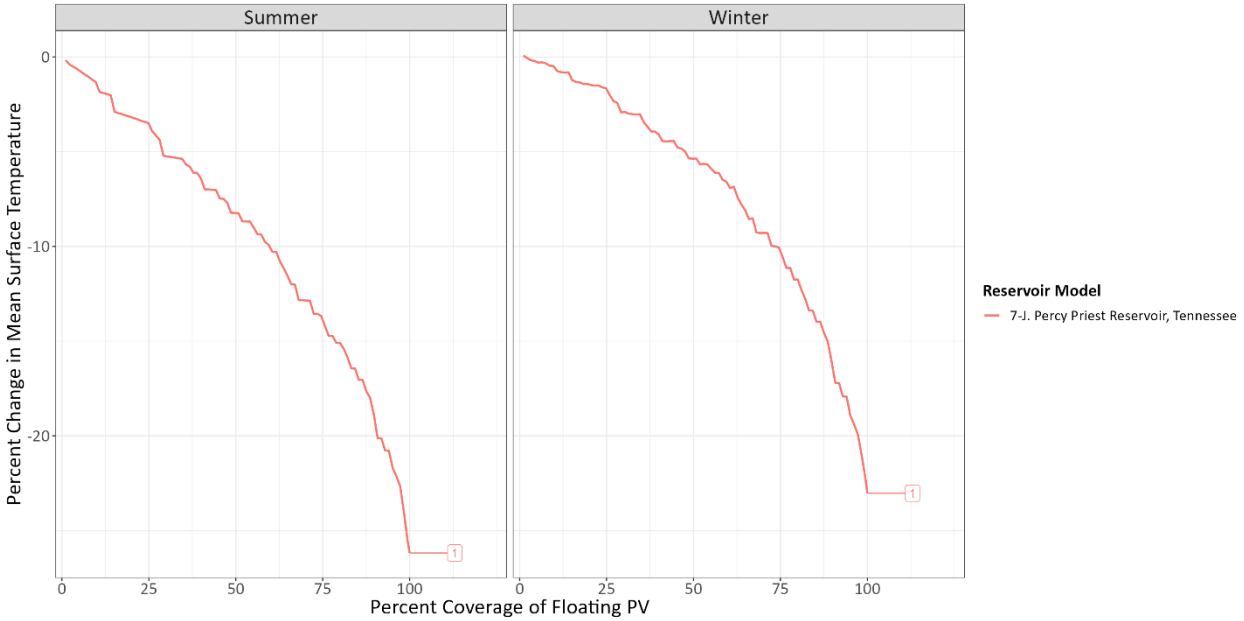

Figure 29. Graph of percent change in average surface temperature for J. Percy Priest Reservoir, Tennessee, across different FPV coverages. Percent change is relative to a reference model with no FPV coverage. Summer months of July and August are separated from winter months of January and February. Positive values indicate a warming surface temperature.

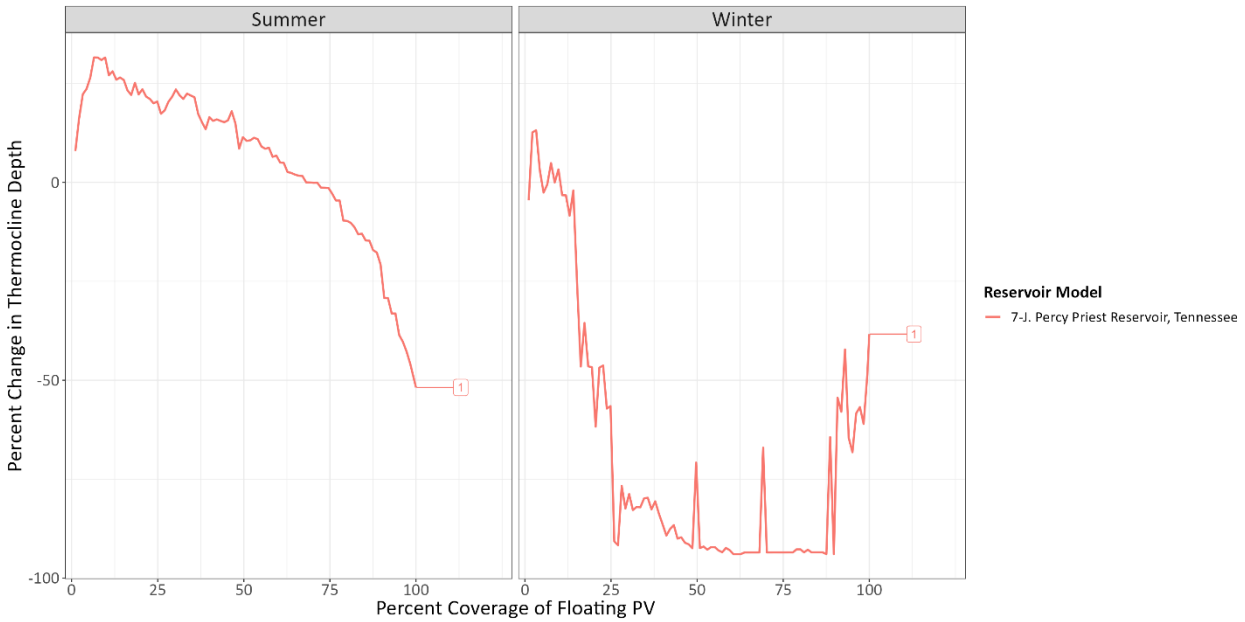

Figure 30. Graph of percent change in thermocline depth for J. Percy Priest Reservoir, Tennessee, across different FPV coverages. Percent change is relative to a reference model with no FPV coverage. Summer months of July and August are separated from winter months of January and February. Positive values indicate a deeper thermocline.

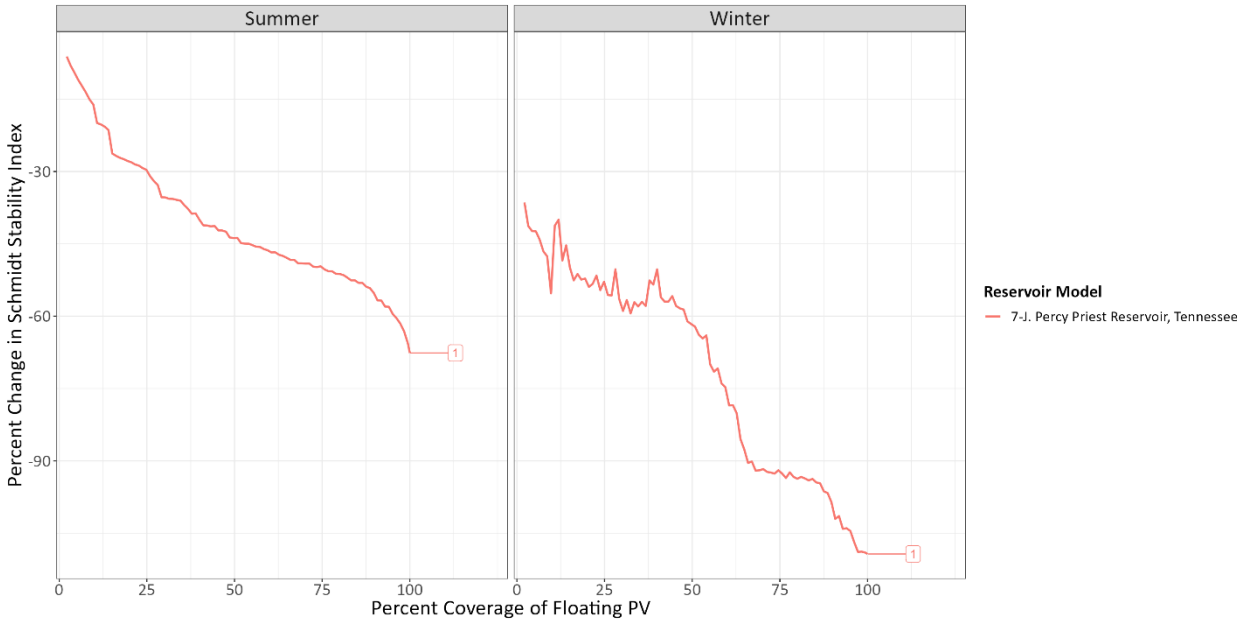

Figure 31. Graph of percent change in Schmidt Stability Index, a measure of stratification strength, for J. Percy Priest Reservoir, Tennessee, across different FPV coverages. Percent change is relative to a reference model with no FPV coverage. Summer months of July and August are separated from winter months of January and February. Positive values indicate a more energy needed to mix water layers, which could be a strong stratification state.

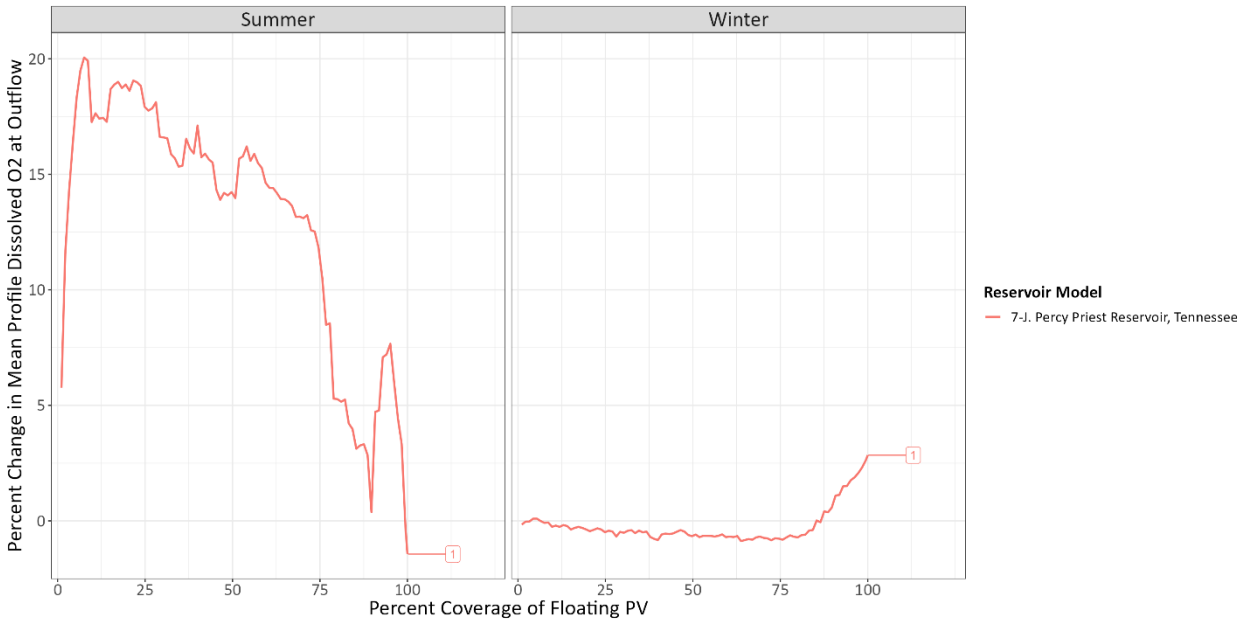

Figure 32. Graph of percent change in dissolved oxygen for J. Percy Priest Reservoir, Tennessee, across different FPV coverages. The average is taken from the vertical profile of the most downstream segment from reservoir model. Percent change is relative to a reference model with no FPV coverage. Summer months of July and August are separated from winter months of January and February. Positive values indicate more DO in the vertical profile.

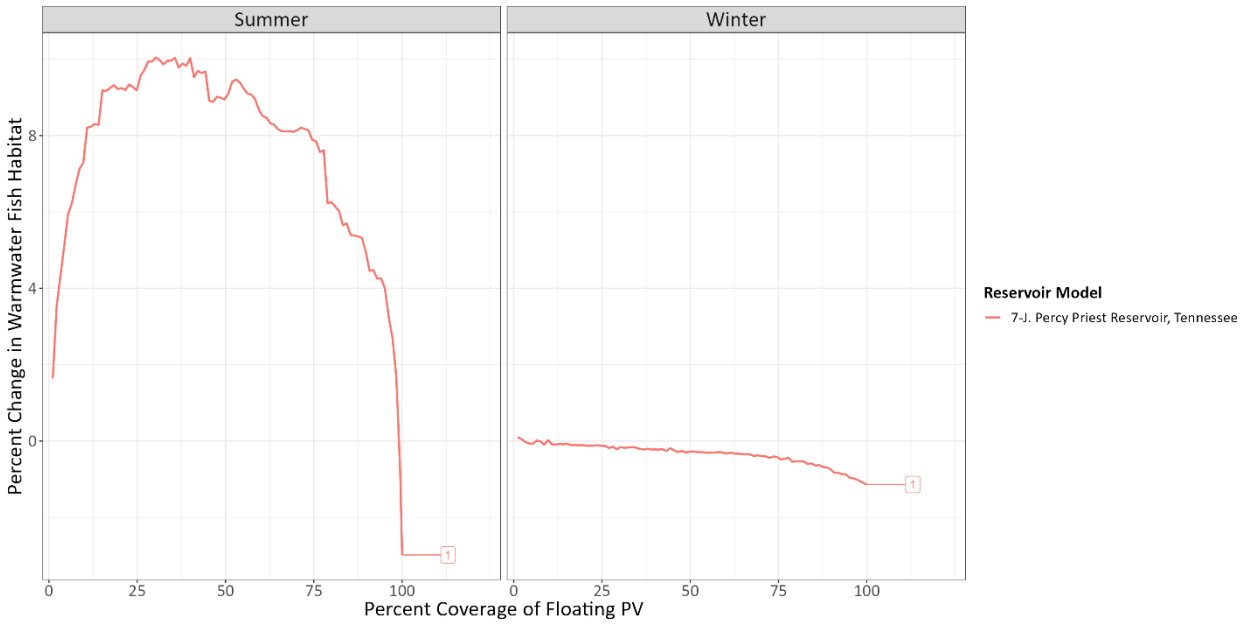

Figure 33. Graph of percent change in potential warmwater fish habitat volume for J. Percy Priest Reservoir, Tennessee, across different FPV coverages. Habitat volumes are determined using an intersection of appropriate thermal range and require dissolved oxygen levels. Percent change is relative to a reference model with no FPV coverage. Summer months of July and August are separated from winter months of January and February. Positive values indicate more potential habitat volume.

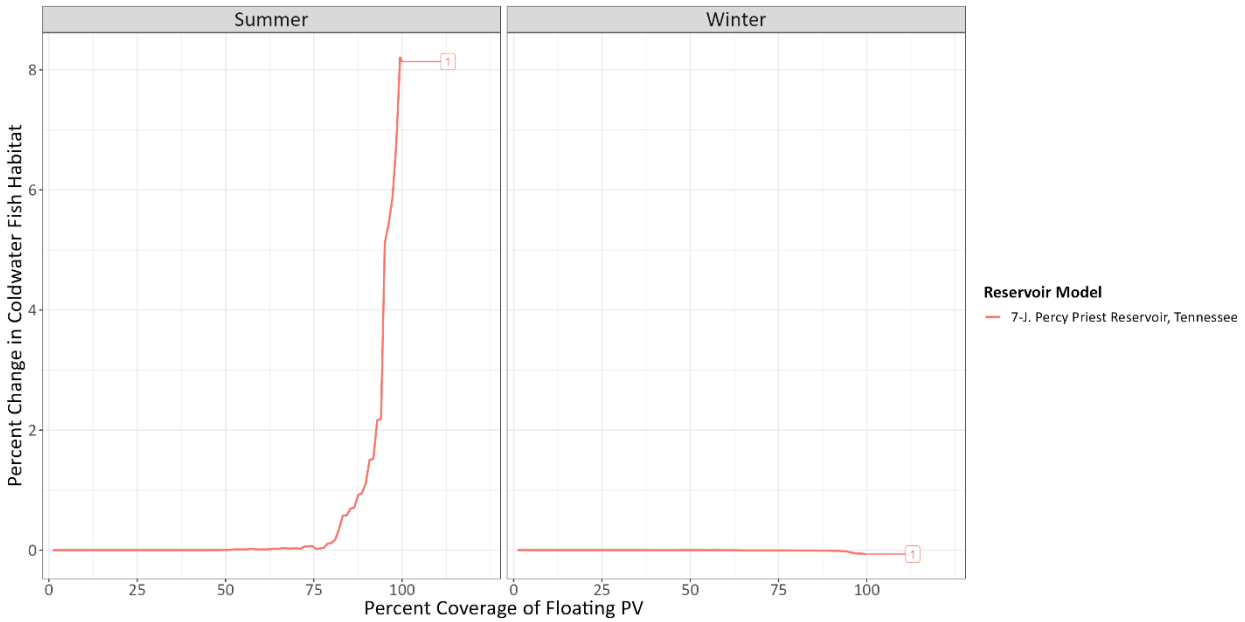

Figure 34. Graph of percent change in potential coldwater fish habitat volume for J. Percy Priest Reservoir, Tennessee, across different FPV coverages. Habitat volumes are determined using an intersection of appropriate thermal range and require DO levels. Percent change is relative to a reference model with no FPV coverage. Summer months of July and August are separated from winter months of January and February. Positive values indicate more potential habitat volume.

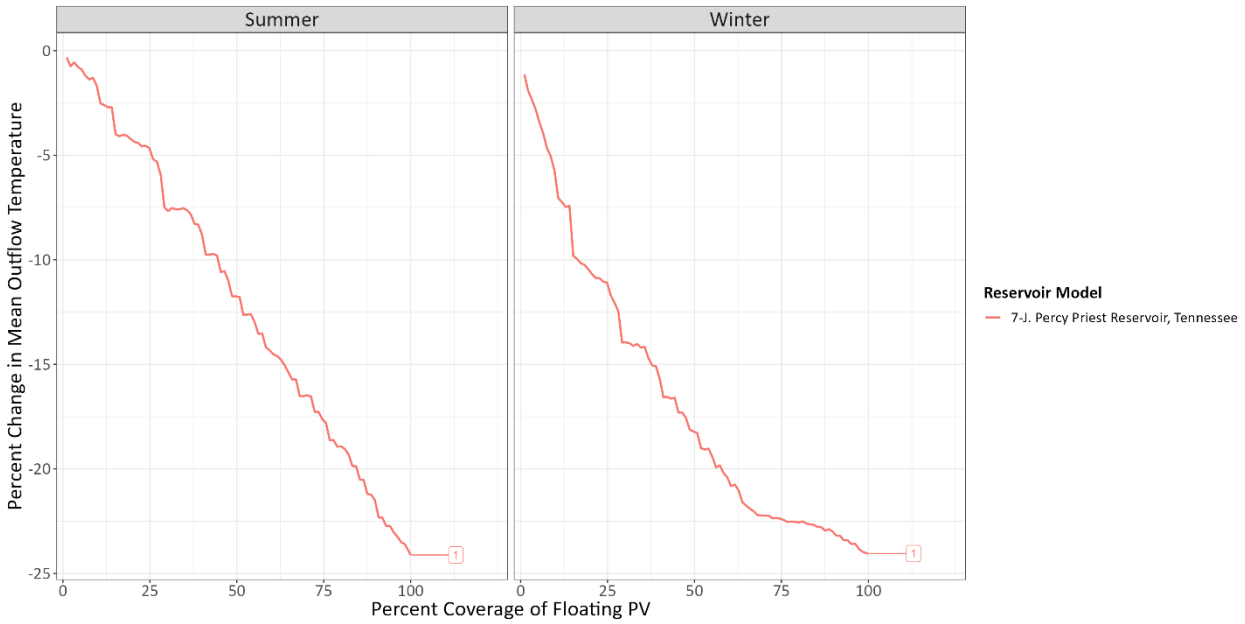

Figure 35. Graph of percent change in outflow water temperature (downstream of dam) from J. Percy Priest Reservoir, Tennessee, across different FPV coverages. Percent change is relative to a reference model with no FPV coverage. Summer months of July and August are separated from winter months of January and February. Positive values indicate warmer outflow water temperature.

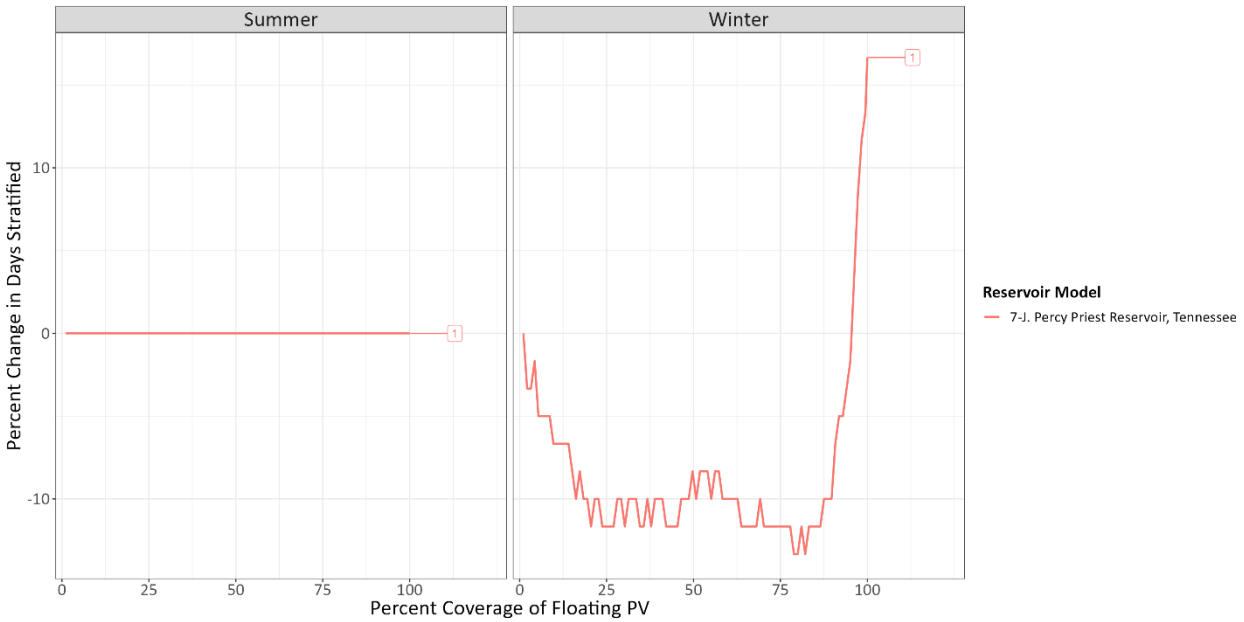

Figure 36. Graph of percent change in the number of days in a stratified state for J. Percy Priest Reservoir, Tennessee, across different FPV coverages. Percent change is relative to a reference model with no FPV coverage. Summer months of July and August are separated from winter months of January and February. Positive values indicate more days stratified during the focal window.

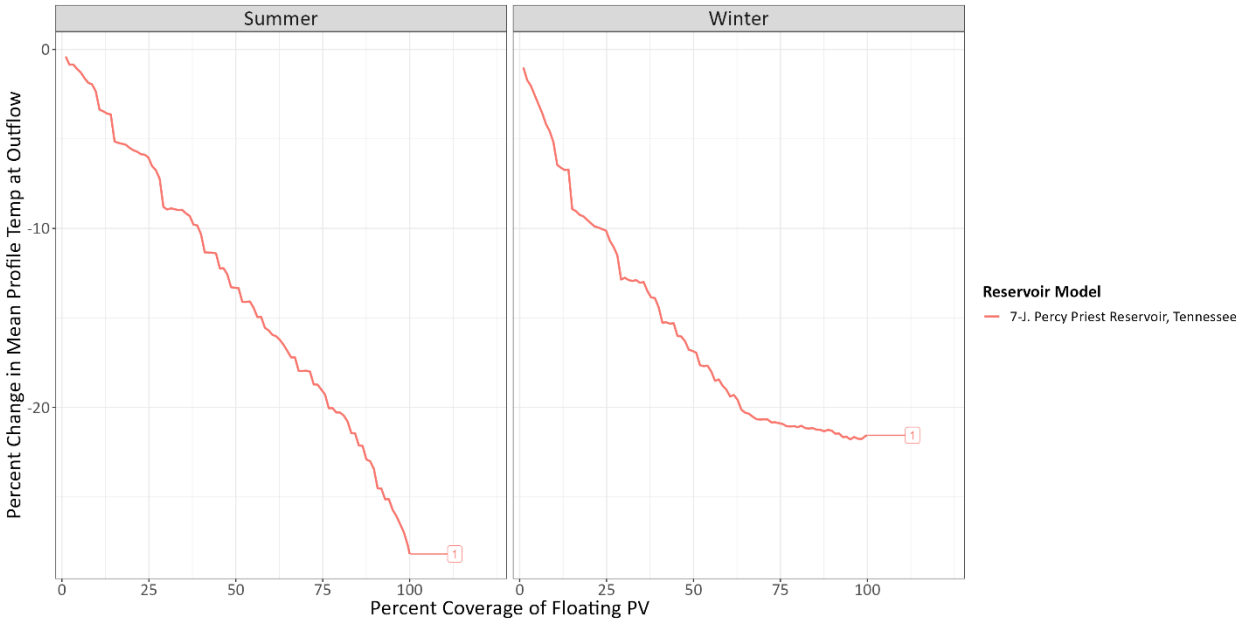

Figure 37. Graph of percent change in mean water temperature of a vertical profile for J. Percy Priest Reservoir, Tennessee, across different FPV coverages. The average is taken from the vertical profile of the most downstream segment from reservoir model. Percent change is relative to a reference model with no FPV coverage. Summer months of July and August are separated from winter months of January and February. Positive values indicate a warmer average temperature of the vertical profile.

4. CONCLUSION

This report underscores the significant potential for integrating FPV with hydropower reservoirs across the continental United States. While there are promising opportunities, particularly in enhancing DO levels and potentially improving compliance with existing hydropower licenses, the current capital costs of FPV are not yet competitive with traditional land-based solar installations when comparing the LCOE results unless the and ITC of 30% is applied and a reduction of 5% from baseline CAPEX is considered. The case study in North Carolina highlighted the importance of location-specific factors, such as irradiance and transmission capacity, which can significantly impact the feasibility and economic viability of FPV projects. Furthermore, the environmental modeling, though largely theoretical due to the nascent stage of large-scale FPV deployment, suggests minimal negative impacts on fish habitats and DO levels, with some potential benefits.

Future work should focus on validating these environmental models through real-world FPV installations and considering broader factors such as recreation, historical preservation, and community water needs. Additionally, a more holistic investigation that includes the hybridization of FPV with hydropower and batteries, along with the long-term environmental effects would be an interesting exercise. The development of more comprehensive CAPEX tools that include a wider range of vendors will also be crucial for accurately estimating costs and supporting stakeholders in making informed decisions about FPV investments.

5. REFERENCES

Atikah, Rifa Hasna, Ni Putu Sri Wahyuningsih, Nyoman Suwartha, and Eko Adhi Setiawan. 2024. "Spatial Analysis of Water Quality Parameters Concentration around the Floating Solar Panel Installation in Lake Mahoni, Depok, Indonesia." E3S Web of Conferences 485: 01010. https://doi.org/10.1051/e3sconf/202448501010.

Bączkiewicz, A. and J. Wątróbski. 2023. "Selection of Floating Photovoltaic System Considering Strong Sustainability Paradigm using SSP-COPRAS Method." In: Proceedings of the 18th Conference on Computer Science and Intelligence Systems, https://doi.org/10.15439/2023f492.

Bax, Vincent, Wietse I. van de Lageweg, Rik Hoosemans, and Bas van den Berg. 2023. "Floating Photovoltaic Pilot Project at the Oostvoornse Lake: Assessment of the Water Quality Effects of Three Different System Designs." Energy Reports 9: 1415–25. https://doi.org/10.1016/j.egyr.2022.12.080.

Benjamins, S., et al. 2024. "Potential Environmental Impacts of Floating Solar Photovoltaic Systems." Renewable and Sustainable Energy Reviews, 199: 114463. https://doi.org/10.1016/j.rser.2024.114463.

Burleyson, Casey, et al. 2023. "Projections of Hourly Meteorology by Balancing Authority Based on the IM3/HyperFACETS Thermodynamic Global Warming (TGW) Simulations." MSD Live. https://doi.org/10.57931/1960530.

Buto, S. G., and R. Anderson. 2020. "NHDPlus High Resolution (NHDPlus HR)—A Hydrography Framework for the Nation." In Fact Sheet (2020–3033). U.S. Geological Survey. https://doi.org/10.3133/fs20203033.

Catania, M., A. Bamoshmoosh, V. Dipierro, M. Ficili, A. Fusco, D. Gioffré, A. Zelaschi, et al. 2024. "Improving the Performance of a Pumped Hydro Storage Plant Through Integration with Floating Photovoltaic." Energy Proceedings 39. https://doi.org/10.46855/energy-proceedings-10909.

"CE-QUAL-W2 Hydrodynamic and Water Quality Model." 2024. https://www.ce.pdx.edu/w2/.

Cube Hydro Carolinas. (n.d.). "Lake Elevation Data." Accessed November 27, 2024. https://cubecarolinas.com/lake-levels/.

Deilami, S., H. Ozgoli, L. Callegaro, S. Taghizadeh, and K. Kim. 2024. "Floating Photovoltaic Solar in Australia: A Feasibility Study." J. Electron. Electric. Eng. 3(2). https://doi.org/10.37256/jeee.3220245731.

Dobos, A. 2014. PVWatts Version 5 Manual. NREL/TP-6A20-62641. https://doi.org/10.2172/1158421.

Eagle Creek Renewable Energy. n.d. "Yadkin River Hydroelectric Project." Accessed March 28, 2025. https://www.eaglecreekre.com/facilities/operating-facilities/yadkin-river-hydroelectric-project

Esparza, I., Á. Candela, L. Huang, Y. Yang, C. Budiono, S. Riyadi, Z. Luo. 2024. "Floating PV Systems as an Alternative Power Source: Case Study on Three Representative Islands of Indonesia." Sustainability 16(3): 1345. https://doi.org/10.3390/su16031345

Exley, Giles, Alona Armstrong, Trevor Page, and Ian D. Jones. 2021. "Floating Photovoltaics Could Mitigate Climate Change Impacts on Water Body Temperature and Stratification." Solar Energy 219: 24–33. https://doi.org/10.1016/j.solener.2021.01.076.

Exley, G., R.R. Hernandez, T. Page, M. Chipps, S. Gambro, M. Hersey, R. Lake, et al. 2021. Scientific and Stakeholder Evidence-based Assessment: Ecosystem Response to Floating Solar Photovoltaics and Implications for Sustainability." Renewable and Sustainable Energy Reviews 52: 111639. https://doi.org/10.1016/j.rser.2021.111639.

Fadliondi, F., B. Budiyanto, P. Chamdareno, P. 2023. "The Improvement Of Solar Panel Performance Using Cooling Method." Trends in Sciences 20(11): 6710. https://doi.org/10.48048/tis.2023.6710.

FERC. Order Issuing New License. Issued September 22, 2016. Alcoa Power Generating, Inc. Project No. 2197-073.

Fick, Stephen E., and Robert J. Hijmans. 2017. "WorldClim 2: New 1-Km Spatial Resolution Climate Surfaces for Global Land Areas." International Journal of Climatology 37 (12): 4302–15. https://doi.org/10.1002/joc.5086.

Goswami, A., P. Sadhu, U. Goswami, P. Sadhu. 2019. "Floating Solar Power Plant for Sustainable Development: A Techno-economic Analysis." Environmental Progress and Sustainable Energy, 38(6). https://doi.org/10.1002/ep.13268

Henkel, S.K., F. Conway, G. Boehlert. 2013. "Environmental and Human Dimensions of Ocean Renewable Energy Development." Institute of Electrical and Electronics Engineers 101(4): 991–998.

Ilgen, Konstantin, Dirk Schindler, Stefan Wieland, and Jens Lange. 2023. "The Impact of Floating Photovoltaic Power Plants on Lake Water Temperature and Stratification." Scientific Reports 13(1): 7932. https://doi.org/10.1038/s41598-023-34751-2.

INL. n.d. "Solar Generation Estimation Tool." AquaPV. Accessed March 28, 2025. https://aquapv.inl.gov/Solar

IRENA (2024); Nemet (2009); Farmer and Lafond (2016) – with major processing by Our World in Data. "Solar photovoltaic module price" [dataset]. IRENA, "Renewable Power Generation Costs"; Nemet, "Interim monitoring of cost dynamics for publicly supported energy technologies"; Farmer and Lafond, "How predictable is technological progress?" [original data]. Retrieved April 8, 2025 from https://ourworldindata.org/grapher/solar-pv-prices

Jasiński, Tomasz. 2020. "Use of New Variables Based on Air Temperature for Forecasting Day-Ahead Spot Electricity Prices Using Deep Neural Networks: A New Approach." Energy 213(C).

Klure, J., T. Hampton, G. McMurray, G., Boehlert, S. Henkel, A. Copping, S. Kramer, et al. 2012. "West Coast Environmental Protocols Framework: Baseline and Monitoring Studies." U.S. Department of the Interior, Bureau of Ocean Energy Management. OCS Study BOEM 2012-013.

Levine, Aaron, Taylor L. Curtis, Ligia E.P. Smith, and Katie DeRose. 2024. "AquaPV: Regulatory and Environmental Considerations for Floating Photovoltaic Projects Located on Federally Controlled Reservoirs in the United States." Golden, CO: National Renewable Energy Laboratory. NREL/TP-6A20-86325. https://www.nrel.gov/docs/fy24osti/86325.pdf.

Lima, Rui L. Pedroso de, Katerina Paxinou, Floris C. Boogaard, Olof Akkerman, and Fen-Yu Lin. 2021. "In-Situ Water Quality Observations under a Large-Scale Floating Solar Farm Using Sensors and Underwater Drones." Sustainability 13(11): 6421. https://doi.org/10.3390/su13116421.

Liu, Zhao, Chao Ma, Xinyang Li, Zexing Deng, and Zhuojun Tian. 2023. "Aquatic Environment Impacts of Floating Photovoltaic and Implications for Climate Change Challenges." Journal of Environmental Management 346:118851. https://doi.org/10.1016/j.jenvman.2023.118851.

Ma, Chao, Runze Wu, and Hui Su. 2021. "Design of Floating Photovoltaic Power Plant and Its Environmental Effects in Different Stages: A Review." Journal of Renewable and Sustainable Energy 13(6): 062701. https://doi.org/10.1063/5.0065845.

McMurray, G.R. 2008. "Wave Energy Ecological Effects Workshop Ecological Assessment Briefing Paper." NOAA Tech. Memo. NMFS-F/SPO-92, pp. 25–66

Mumtaz, A., S. Kazmi, A. Altamimi, Z. Khan, S. Alyami. 2024. "Multi-dimensional Potential Assessment of Grid-connected Mega-scale Floating PV Power Plants Across Heterogeneous Climatic Zones." Frontiers in Energy Research, 12. https://doi.org/10.3389/fenrg.2024.1404777.

Nobre, R., S. Boulêtreau, F. Colas, F., Azémar, L. Tudesque, N. Parthuisot, P. Favriou, and J. Cucherousset. 2023. "Potential Ecological Impacts of Floating Photovoltaics on Lake Biodiversity and Ecosystem Functioning." Renewable and Sustainable Energy Reviews 188: 113852. https://doi.org/10.1016/j.rser.2023.113852.

NREL. 2024. "Utility Scale PV." Annual Technology Baseline. Accessed March 27, 2025. https://atb.nrel.gov/electricity/2024/utility-scale_pvRai, A., A. Timilsina, B. Nepali. 2020. "Overview and Feasibility of Floating Solar Photovoltaic System in Nepal." Journal of the Institute of Engineering 15(3), 267–274. https://doi.org/10.3126/jie.v15i3.32194

Silalahi, David Firnando, and Andrew Blakers. 2023. "Global Atlas of Marine Floating Solar PV Potential." Solar 3(3): 416–33. https://doi.org/10.3390/solar3030023.

Solomin, E., E. Sirotkin, E., Cüce, S. Priya, K. Sudhakar. 2021. "Hybrid Floating Solar Plant Designs: A Review." Energies 14(10): 2751. https://doi.org/10.3390/en14102751

Steyaert, J. C., L. E. Condon, S. W. D. Turner, N. Voisin. 2022. "ResOpsUS, A Dataset of Historical Reservoir Operations in the Contiguous United States." Scientific Data 9(34). https://doi.org/10.1038/s41597-022-01134-7.

Sukarso, A., K. Kim. 2020. "Cooling Effect on the Floating Solar PV: Performance and Economic Analysis on the Case of West Java Province in Indonesia." Energies 13(9): 2126. https://doi.org/10.3390/en13092126.

Sun, M., T. B. Phillips, T. Hussain and J. Gallego-Calderon. 2024. "Techno-Economic Assessment of Electricity Market Potential for Co-Located Hydro-Floating PV Systems." 2024 IEEE Green Technologies Conference (GreenTech), Springdale, Arkansas. https://doi.org/10.1109/GreenTech58819.2024.10520558.

U.S. Environmental Protection Agency (EPA). 1998. "Guidelines for Ecological Risk Assessment." 630/R-95/002F.

U.S. EPA. 2014. "NHDPlus (National Hydrography Dataset Plus)." Accessed March 18, 2025. https://www.epa.gov/waterdata/nhdplus-national-hydrography-dataset-plus.

Venturini, P., G. Gagliardi, G., Agati, L. Cedola, M. Caputi, D. Borello. 2024. "Integration of Floating Photovoltaic Panels with an Italian Hydroelectric Power Plant." Energies 17(4): 851. https://doi.org/10.3390/en17040851.

Wu, S., N. Jiang, S. Zhang, P. Zhang, P., Zhao, Y. Liu, Y. Wang. 2024. "Discussion on the Development of Offshore Floating Photovoltaic Plants, Emphasizing Marine Environmental Protection." Frontiers in Marine Science 11. https://doi.org/10.3389/fmars.2024.1336783.

Yang, P., L. Chua, K. Irvine, M. Nguyen, E. Low. 2022. "Impacts of a Floating Photovoltaic System on Temperature and Water Quality in a Shallow Tropical Reservoir." Limnology 23(3): 441–454. https://doi.org/10.1007/s10201-022-00698-y.

Ziar, Hesan, Bjorn Prudon, Fen-Yu (Vicky) Lin, Bart Roeffen, Dennis Heijkoop, Tim Stark, Sven Teurlincx, et al. 2021. "Innovative Floating Bifacial Photovoltaic Solutions for Inland Water Areas." Progress in Photovoltaics: Research and Applications 29(7): 725–43. https://doi.org/10.1002/pip.3367.